

SEX DIFFERENCES IN THE FEMUR AND ACETABULUM: BIOMECHANICAL
ANALYSIS WITH FORENSIC SIGNIFICANCE

by

Maureen W. Purcell, B.A.

A thesis submitted to the Graduate Council of
Texas State University in partial fulfillment
of the requirements for the degree of
Master of Arts
with a Major in Anthropology
December 2013

Committee Members:

Daniel J. Wescott, chair

M. Kate Spradley

Michelle D. Hamilton

COPYRIGHT

by

Maureen W. Purcell

2013

FAIR USE AND AUTHOR'S PERMISSION STATEMENT

Fair Use

This work is protected by the Copyright Laws of the United States (Public Law 94-553, section 107). Consistent with fair use as defined in the Copyright Laws, brief quotations from this material are allowed with proper acknowledgment. Use of this material for financial gain without the author's express written permission is not allowed.

Duplication Permission

As the copyright holder of this work I, Maureen W. Purcell, authorize duplication of this work, in whole or in part, for educational or scholarly purposes only.

ACKNOWLEDGEMENTS

I would like to thank my committee chair and advisor, Dr. Wescott, for his insight, encouragement, and guidance regarding my thesis project. I also want to thank my committee members, Dr. Hamilton and Dr. Spradley, for their edits and advice in the development of my thesis.

Thank you to Dr. Steadman at the University of Tennessee-Knoxville for allowing me to utilize the William Bass Collection for my research. Thank you to Sophia Mavroudas for permission to collect data from the Texas State University Donated Collection.

Finally, thank you to all the individuals who donated their remains to the Texas State and University of Tennessee collections.

TABLE OF CONTENTS

ACKNOWLEDGEMENTS	iv
LIST OF TABLES	vi
LIST OF FIGURES	vii
ABSTRACT	x
CHAPTER	
I. INTRODUCTION.....	1
Pelvis Morphology	3
Femur Morphology	4
Sexual Dimorphism in the Pelvis and Femur	9
Research Questions	12
Null Hypotheses.....	12
II. MATERIALS AND METHODS.....	14
Sample.....	14
Landmark Data.....	14
Calculation of Measurements and Angles from 3D	
Coordinate Data	22
Analysis of 3D Data.....	29
III. RESULTS.....	31
Analysis of Lengths and Angles	31
Analysis of Landmark Data	41
Null Hypotheses Results Summary	49
IV. DISCUSSION	51
Conclusion	59
REFERENCES	61

LIST OF TABLES

Table	Page
1.1. Landmarks for the os coxae and left femur	15
1.2. Metric measurements of the os coxae and femur.....	22
1.3. Derived points and axes	25
1.4. Angle measurements	25
2.1. Tests of normality in the pelvis and femur	31
2.2. Tests of sexual dimorphism in measurements and angles	32
2.3. Pearson correlation table for pelvic and femoral measurements	35
2.4. DFA for pelvis and femur	42
2.5. CVA for pelvis and femur.....	42
2.6. Standard canonical coefficients for the femur	49
2.7. Classification results	49
2.8. Summary of null hypotheses tested in this thesis	50

LIST OF FIGURES

Figure	Page
1.1. Metric measurements of pelvis	4
1.2. Bicondylar (oblique) and neck-shaft angles of the femur.....	6
1.3. Femoral angle of version (superior view, anterior is up).....	7
2.1. Articulated pelvis with landmarks (numbers represent landmarks described in Table 1.1).....	17
2.2. Anterior (A) and posterior (B) views of the femur with landmarks (numbers correspond to landmarks defined in Table 1.1)	18
2.3. Acetabulum measurements for landmarks 14-17 on the left os coxa (landmarks 6-9 on right side)	19
2.4. Femoral condyle measurements (numbers represent landmarks defined in Table 1.1	19
2.5 Femur on clay pillars for landmark data collection	20
2.6. Metric measurements for the pelvis (landmarks correspond to those in Table 1.2).....	22
2.7. Metric measurements of the femur with corresponding landmarks.....	23
2.8. Neck-shaft angle, anterior view (corresponding to derived points and axes, and angles in Tables 1.3 and 1.4.....	26
2.9. Femoral angle of version/torsion, superior view, anterior is up (corresponding to derived points and axes, and angles in Tables 1.3 and 1.4)	27

2.10. Bicondylar/oblique angle of the femur, anterior view (corresponding points and axes, and angles in Tables 1.3 and 1.4)	28
3.1. Distribution of male and female biacetabular breadth	33
3.2. Distribution of male and female neck-shaft angle	33
3.3. Distribution of male and female bicondylar angle	34
3.4. Distribution of male and female biomechanical neck length	34
3.5. Regression of neck-shaft angle (degrees) and biacetabular breadth (mm) R ² values: Males 0.061; Females 0.088 Equations: Males $y=99.54+0.24*x$; Females $y=95.51+.24*x$	36
3.6. Regression of bicondylar angle (degrees) and biacetabular breadth (mm) R ² values: Males 0.002; Females 0.128 Equations: Males $y=84.57+0.0048*x$; Females $y=80.7+0.04*x$	37
3.7. Regression of neck shaft angle (degrees) and bicondylar angle (degrees) R ² values: Males 0.354; Females 0.121 Equations: Males $y=77.2+0.06*x$; Females $y=79.92+0.05*x$	38
3.8. Regression of bicondylar angle (degrees) and biomechanical neck length (mm) R ² values: Males 0.135; Females 0.066 Equations: Males $y=88.54+-0.04*x$; Females $y=87.83+-0.04*x$	39
3.9. Regression of neck-shaft angle and biomechanical neck length R ² values: Males 0.127; Females 0.041 Equations: Males $y=146+-0.24*x$; Females $y=152+-0.36*x$	40

3.10. PC1 of Landmark differences between females and males in the femur	
(Landmark numbers correspond to those in Table 1.1).....	43
3.11. PC2 of Landmark differences between females and males in the	
femur (Landmark numbers correspond to those in Table 1.1)	44
3.12. PC1 shape differences between females and males in the pelvis in the	
anterior view (Landmark numbers correspond to those in Table 1.1).....	45
3.13. PC2 shape differences between females and males in the pelvis in the	
anterior view (Landmark numbers correspond to those in Table 1.1).....	45
3.14. PC1 shape changes between females and males in the pelvis in the superior	
view, posterior is up (landmark numbers correspond to those in Table 1.1)	46
3.15. PC2 shape changes between females and males in the pelvis in the superior	
view, posterior is up (landmark numbers correspond to those in Table 1.1)	46
3.16. PC1 and PC2 graph for the femur in females (gray) and males (black)	47
3.17. PC1 and PC2 graph for the pelvis in females (gray) and males (black)	48

ABSTRACT

Knowing the relationship between pelvic and femur morphology is essential for understanding femoral developmental plasticity, sexual dimorphism, and morphological changes associated with habitual load levels. The purpose of this Master's thesis is to examine how pelvic dimensions influence the shape of the femur within a biomechanical framework in a modern American White population. Specifically the research examines the relationship between sex differences in biacetabular breadth and femoral functional angles, and whether these differences are significant enough to provide a forensically relevant equation for estimating sex with the femur. Sexual dimorphism in pelvic dimensions and femoral angles of 30 males and 30 females were analyzed using landmarks on a 3D Cartesian coordinate system with geometric morphometric techniques to provide a visual representation of overall shape change in the femur and pelvis between males and females. A Principle Component Analysis (PCA) with Procrustes coordinates revealed significant shape differences in epicondylar breadth, acetabular version, and iliac flare between males and females. Analysis of the raw metric data also showed significant sexual dimorphism in the biacetabular breadth, biomechanical neck length, femoral neck-shaft angle, femoral angle of version, and the bicondylar angle. A Discriminant Function Analysis (DFA) was utilized for the forensic application component with a classification percentage of 85, with a stepwise procedure. Regression analysis demonstrated significant relationships to exist between several variables, including biacetabular breadth, the neck-shaft angle, and the bicondylar angle. The

findings also show that the neck-shaft angle and biomechanical neck length are correlated with the bicondylar dimensions. Overall, this research indicates that the femoral and pelvic morphological traits are multi-factorial and reflect biomechanical adaptations to varying dimensions among humans, which has applications for reconstructing modern and fossil human femoral plasticity and variation.

CHAPTER I

INTRODUCTION

Studies of sexual dimorphism in the femur mostly focus on size differences rather than shape variation, or how the femur functions with the pelvis as a unit. Our understanding of how sex variation in pelvic morphology in a modern population affects the shape of the femur remains relatively unexplored. The purpose of this research is to examine size and shape sexual dimorphism in the femur and pelvis within a biomechanical framework, and how differences in size and shape of the femur correlate with sex differences in pelvic dimensions and shape. Specifically, this thesis addresses the question: do differences in biacetabular breadth in females create significantly different changes in the femur compared to males? A few studies suggest the femoral shape and hip shape might be consistently dimorphic across populations (Albanese et al., 2008; Kurki, 2011; Kurki, 2013). To further examine these differences, a comprehensive analysis must be utilized to understand the relationship between adult pelvic and femoral morphology.

An explanatory analysis was conducted to examine the biomechanically-derived differences in the femur between males and females. An informed investigation of the femoral shape could reveal the relationship between the development of the femur and pelvis as a functional unit. If significant sex differences in the femur are found, a discriminant function equation will be developed to estimate sex for forensic anthropology cases. A discriminant function equation to estimate sex will be helpful in

the event that the os coxae are not recovered or cannot be analyzed. Although a derived discriminant function analysis may be population specific, it provides another method of estimation in the event of taphonomic damage to the femoral head or epicondyles (widths often used for metric sex estimation).

Researchers can also utilize these methods to examine femoral and pelvic shape variation across populations and within the modern human and hominid skeletal collections. The research results will be applicable to paleoanthropological researchers because it will examine the relationship between pelvis breadth and the size and shape of the femur. Bioarchaeological research often examines population-based skeletal variation to examine past lifeways. The methods in this thesis provide a comprehensive way to examine lower limb morphology, which is often utilized to draw conclusions about division of labor, status, and other aspects of culture.

Beyond anthropology, this research adds to the application of skeletal biological knowledge in clinical settings. Orthopedic surgeons often cite sexual dimorphism in the quadriceps angle (Q-angle) between males and females when attempting to explain male and female differences in injury and osteoarthritic risk, but there is disagreement over the empirical evidence of this trait (Byl et al., 2000). This angle has been linked to increased likelihood of patellofemoral pain and the increased work force needed around the hip for a wider pelvis (Binder and Brown-cross, 2001). The increased demand placed on the stabilizing muscles in the hip could possibly reflect statistically significant differences in the femur, not just the pelvis. Illuminating any significant skeletal differences would provide more information for those investigating sex-based variation in pathogenesis and

disease risk. This thesis explores this concept by including landmarks for the muscle attachment sites important for the lever of the hip on the femur and pelvis.

Pelvis Morphology

The pelvis consists of the sacrum and right and left os coxae. The os coxa is composed of three primary centers of ossification present at birth: the ilium, ishium, and pubis. The acetabulum of the os coxa is the facet where the femoral head articulates to form the hip joint. Three epiphyses form in the cartilage that becomes the acetabulum, as the ischium, ilium and pubis form the triradiate area in the acetabulum (Scheuer and Black, 2000). The ischium and pubis fuse together first at the ramus around 5 to 8 years of age (Scheuer and Black, 2000). Fusion of the acetabular region commences at approximately 11 in females and 14 in males and is complete by 15 to 17 years of age (Schuer and Black, 2000). The sacrum is part of the spinal column and articulates with the posterior portion of the ilium and the sacro-iliac joint (SIJ). The sacral primary ossification centers are present at birth and by age 6 all primary centers are fused, with the posterior spinous process joining the bone later between aged 7-15 (Scheur and Black, 2000).

Some of the biomechanically relevant measurements and angles of the pelvis used in this study include biacetabular breadth and bi-iliac breadth (Figure 1.1). Biacetabular breadth is distance between the centers of the left and right acetabulae in an articulated pelvis. Bi-iliac breadth is the distance between the iliac tubercles for an articulated pelvis. Also considered is acetabular version, or the orientation of acetabulum to the sagittal and longitudinal plane, or how “forward-facing” the acetabula appear when viewed anteriorly.

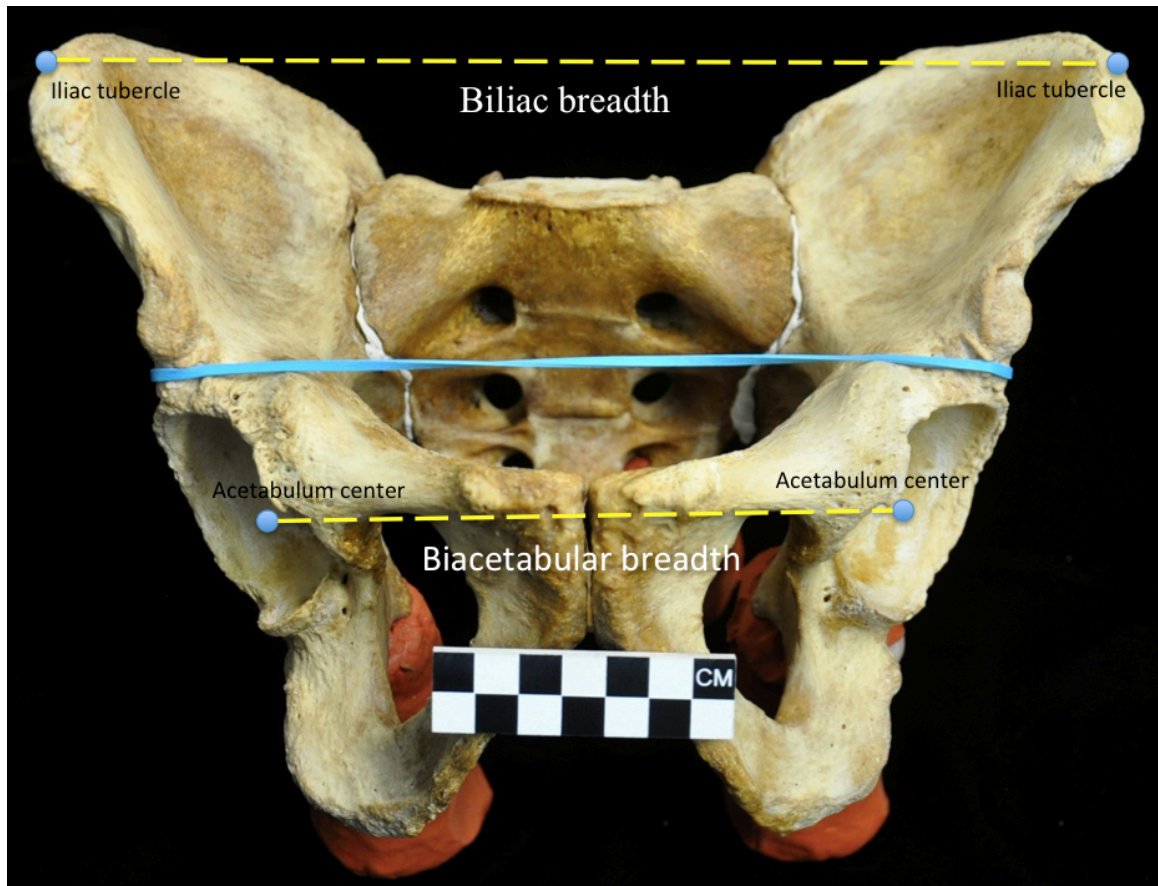


Figure 1.1: Metric measurements of the pelvis

Femur Morphology

The femur is the largest long bone and articulates proximally with the acetabulum of the pelvis and distally with the tibia and patella. Because of its density and size, it is often recovered in bioarchaeological and forensic contexts. The femur provides information about stature and activity, and the head diameter is used for metric sex estimation in some populations (Trotter and Gleser, 1952; Auerbach and Ruff, 2010; Spradley and Jantz, 2011). During development, the head ossifies by the end of the first year and fuses around 16-20 years of age, with females tending to complete growth earlier than males. In the distal epiphyses the condyles ossify in the 9th month *in utero* and fuse a year or two after the head (Scheur and Black, 2000). The fact that this bone is

under a great deal of loading pressure and fuses well after puberty means that differences in gait and activity level affect its morphology during ontogeny. Thus, the prevalence of this bone in the archaeological (and paleoanthropological) record, as well as its responsive and dynamic properties, make it an important bone for analysis.

A popular method of examining variation in femur morphology is by measuring the functional angles of the bone. There are several biomechanically relevant measurements and angles of the femur including the bicondylar (also known as the valgus or oblique angle), neck-shaft, and version (i.e., neck torsion) angles (Figure 1.1-1.2). These angles change during growth and development and also differ among populations as a result of genetic and activity (functional) differences.

The valgus angle orientation of the femur (how the femur angles medially from the hip to the knee) is examined across several fields of science because of its relevance to gait, and this angle is also quantified in multiple ways. Orthopedic literature often cites the Quadriceps-angle (Q-angle) differences between males and females, and it is measured as the angle formed by the intersection of two lines: one from the tibial tuberosity to center of the patella, the other from the center of the patella to the anterior-superior iliac spine (Byl et al., 2000). Paleoanthropologists and bioarchaeologists examine the valgus shape as the bicondylar angle, defined as the angle between an axis through the shaft of the femur and a line perpendicular to the infracondylar plane. Paleoanthropologists extrapolate information about gait and standing posture in hominids from this bicondylar angle and from proximal femoral shape (Ruff, 1995; Holliday et al., 2010).



Figure 1.2: Bicondylar (oblique) and neck-shaft angles of the femur

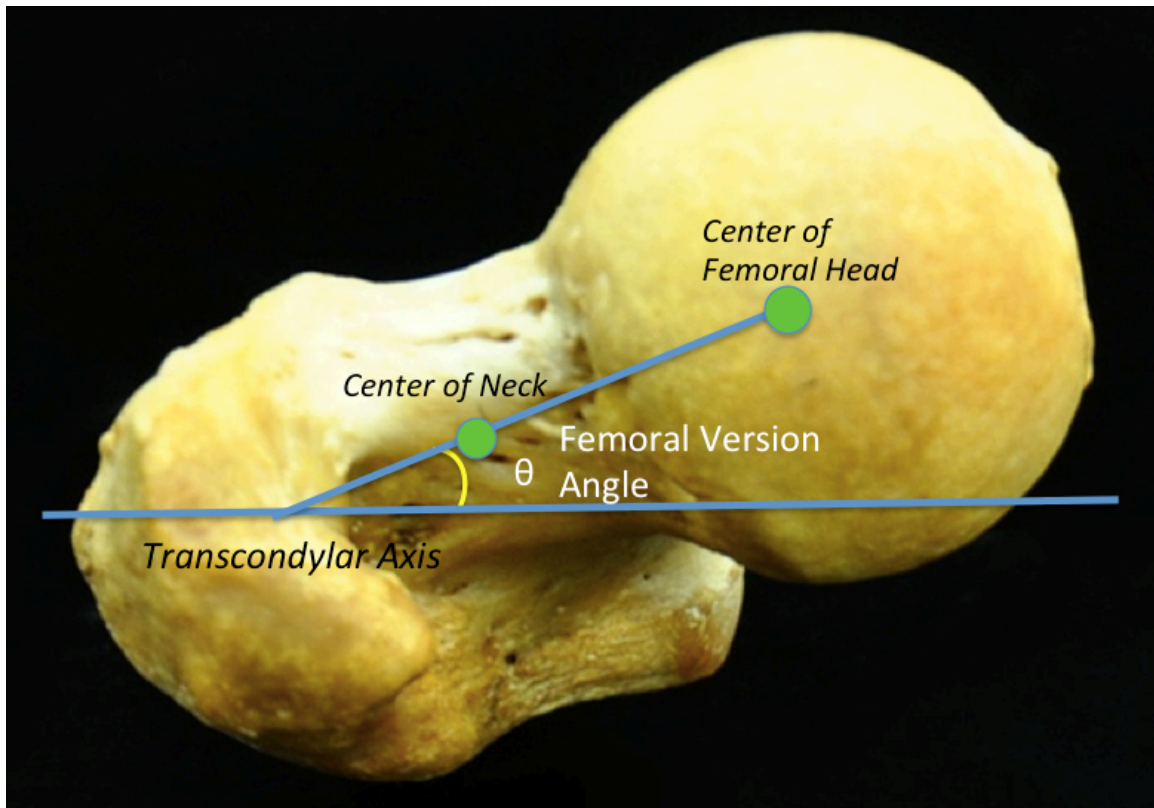


Figure 1.3: Femoral version angle (superior view, anterior is up)

The bicondylar angle has genetic as well as developmental/functional components (Tardieu et al., 2006). Human infants are born with a varus femoral angle causing a bow-legged appearance, and the valgus angle develops at the onset of walking (Salenius and Vankka, 1975). Humans that never develop ambulatory skills do not develop a bicondylar angle (Tardieu, 2010). In addition, the bicondylar angle changes during gait maturation, as the femur is under a biomechanical influence to position the knee close to the body's center of gravity. However, a related structure, the lateral trochlear lip is present in the human fetus, although biomechanically this feature is only functional when the individual is bipedal as it protects against lateral displacement of the patella (Tardieu et al., 2006). Clearly, genetic and developmental influences both impact the formation of this angle and the overall morphology of the femur. This suggests that variations arising from genetically-induced biomechanical differences, such as a wider

biacetabular breadth, are observable on the femur as expressed through sexual dimorphism.

The femoral neck-shaft angle is measured as the angle formed by the meeting of the axis of the line through the center of the femoral head and neck with the long axis of the femur diaphysis. The neck-shaft angle decreases from an average of 160 degrees in early childhood to 125 degrees during adulthood but will decrease to 120 degrees in the elderly (Scheuer and Black, 2000). The decline in neck-shaft angle is dependent on weight-bearing forces, and bioarchaeological studies have noted that the neck-shaft angle differs with subsistence strategies and activity level (Gilligan et al., 2013). Anderson and Trinkaus (1998) found modern urban individuals to have higher neck-shaft angles than historic and prehistoric hunter-gatherer groups, while historic and modern agricultural populations had a mixture of larger and smaller angles. Although they did not find a strong sex differences, their study did not consider femoral length, neck length, or bicondylar angle as a confounding variable. These traits vary across populations and could impact the development of the neck-shaft angle.

Femoral version (angle of torsion) is a measure of the twist between the proximal and distal ends of the femoral diaphysis. Femur version also varies throughout life. At birth, anteversion (a condition in which the femoral neck is twisted anteriorly with respect to the rest of the femur) is normally between 32 and 35 degrees and stabilizes around 8 degrees by adulthood. Although there is variation within and among populations, in general the anteversion angle decreases with skeletal maturity. This is thought to be related to the biomechanical forces imposed on the proximal epiphyseal plates with the onset of walking (Fabeck et al., 2002). The severity of this angle is

susceptible to biomechanical influences throughout development (Tardieu, 2010; Wescott and Cunningham, 2013)

Sexual Dimorphism in the Pelvis and Femur

The nonmetric and metric differences between males and females in the pelvis are well documented (Tardieu and Trinkaus, 1994; Bytheway and Ross, 2010; Phenice, 1969; Tardieu et al., 2006). Nonmetric characteristics include, but are not limited to, the ventral arc, ishiopubic ramus morphology, pubic angle, sciatic notch shape, and auricular surface elevation. Biacetabular breadth in particular is noted as a consistently dimorphic metric trait, with females having a wider pelvis relative to body size to enlarge the birth canal (Kurki, 2007; Kurki, 2011; Schuer and Black, 2000). However, the majority of these studies utilize archaeological or early hominid samples. Driscoll (2010) examined secular change of the pelvis across both historical and modern White and Black populations over the past 140 years, noting that the overall secular trend was a narrowing of the pelvis.. Therefore, an examination of a modern skeletal population using methods available to most anthropologists is necessary to determine how these dimorphic traits might affect femoral development in modern populations.

Bytheway and Ross (2010) performed an overall landmark geometric morphometric analysis of the os coxae but did not examine biacetabular breadth. Their results indicated that expected variation in the ilium and pubic symphyseal area occurred, with males having a more flared ilium, and females displaying a more medially-placed symphysis. The differences in the acetabulum were not found to be significant, however a lateral point on the acetabulum was not taken. This would be the area where any possible pelvic or acetabular anteversion would be most pronounced, therefore it is

possible sex differences in acetabular version were present, but not observed. In fact, Tohtz et al. (2010) found significant sex differences in anteversion in living humans through MRI in 69 females and 72 males. Overall, females exhibited more anteverted acetabula, and these results were significant enough for the authors to suggest the need for sex-specific hip replacements.

The degree of size sexual dimorphism in biacetabular breadth varies among populations (Tardieu and Trinkaus, 1994). However, the dimorphism observed is not tied to differences in body size, therefore an examination of shape differences is essential to examine sex variation in femoral morphology (Kurki, 2011). Population differences appear to be consistent with the evolutionary necessity for a wide birth canal, but there is variation in shape among populations (Kurki, 2013), and this study will control for population as best as possible.

American Whites, generally understood to be of western European descent, were the population utilized for this analysis. Any resulting developmental differences in the femora between males and females may display a consistent pattern among populations. However, this is not confirmed and is only an assumption. This research will help begin to address the biomechanically-driven variations that might exist by controlling for population.

One-dimensional measurements of the femur capturing the breadth or length of anatomical features are used extensively in forensic anthropological studies to develop population-specific sex estimations (Jantz et al., 2008; Srivastava et al., 2011; Stull and Godde, 2012). However, biomechanical studies can provide a much better explanation of the cause of variation in femur sexual dimorphism. For example, the wider biacetabular

breadth in females is cited as a reason for observed smaller neck-shaft angles in females than males (Standring, 2008). Females also often possess comparatively shorter necks and greater angles of femoral version (Traina et al., 2009). The femoral neck-shaft angle, however, does not exhibit consistent sexual dimorphism (Nakahara et al., 2011; Traina et al., 2009; Gilligan et al., 2013), but many of the studies focusing on femoral neck-shaft angle have included elderly individuals or those with preexisting pathologies.

Furthermore, recent literature has indicated that there is a need to examine population differences in femur morphology for arthroplasty purposes (Baharuddin et al., 2013).

Although metric sex estimation is possible with the femur, the overall morphology of shape-based sexual dimorphism has received less attention. Albanese (2008) provided a metric sex estimation technique on the femur, focusing on the triangulation of the greater trochanter to the lesser trochanter to the fovea capitis. Tests on an independent sample pointed to an accuracy of 95-97%. However, Albanese (2008) did not separate the sample by ancestry because his aim was to provide a non-population specific sex estimation equation. There was no examination of the pelvis, however, so any biomechanical explanation of this dimorphism is speculative. Albanese (2008) provided a working equation for sex estimation, but it has not been independently tested across populations. Furthermore, without a complete examination of femoral shape and corresponding pelvis the possible mechanisms behind this dimorphism are unknown, and it is also unknown if these landmarks are the best to estimation sex.

Sexual dimorphism and shape differences do exist in the pelvis, and population-specific size dimorphism does exist in the femur (Kimmerle et al., 2008; Spradley and Jantz, 2011). Shape changes resultant from sex-related biomechanical differences in the

pelvis is likely, and there is some literature supporting this conclusion (Weidow 2006; Tohtz, 2010; Nakahara et al., 2011). However, quantitative analysis correlating the shape changes in the os coxae and femur within one individual or multiple individuals within a known population has not been performed to the author's knowledge. Furthermore, a comprehensive methodology useful for forensic anthropologists, bioarchaeologists and paleoanthropologists will allow for better understanding of the dimorphism of these shape changes, and any possible variation across populations.

Research Questions

The main focus of this study is to investigate how the sexual dimorphism in the pelvis contributed to sex differences in femur shape and size. Therefore, the null hypotheses will examine the variation between males and females. Also, correlation in the variation within each sex between the pelvis and femur was examined.

Null Hypotheses

- H₀1: There is no significant sexual dimorphism in biacetabular breadth.
- H₀2: There is no significant sexual dimorphism in the bi-iliac breadth.
- H₀3: There is no significant sexual dimorphism in the biomechanical neck length.
- H₀4: There is no significant sexual dimorphism in the femoral angle of version.
- H₀5: There is no significant sexual dimorphism in overall femoral shape and morphology
- H₀6: There is no significant sexual dimorphism in the neck-shaft angle.
- H₀7: There is no significant sexual dimorphism in the femoral bicondylar angle.
- H₀8: There is no significant sexual dimorphism in overall pelvic shape and morphology

- H₀9: There is no significant sexual dimorphism in the acetabular angle of version.
- H₀10: There is no significant relationship between the biacetabular breadth and the femoral neck-shaft angle.
- H₀11: There is no significant relationship between the biacetabular breadth and the femoral bicondylar angle.
- H₀12: There is no significant relationship between the biomechanical neck length and the femoral bicondylar angle.

CHAPTER II

MATERIALS AND METHODS

Sample

Morphometric landmark data of the pelvis and femur were recorded for 30 males (mean age, age range) and 30 females (mean age, age range) classified as American Whites. The selection of individuals from a single ancestral group helps control for possible population differences in variation. Paired pelvises and femora with significant pathologies, such as hip and knee replacements, femur fractures, or joint infections were not included in the study. The sample includes human remains from two different collections: the Texas State Donated Skeletal Collection at Texas State University (n = 20) and the William M. Bass Donated Skeletal Collection at the University of Tennessee at Knoxville (n = 40). These collections contain skeletal remains of modern individuals whose bodies were donated by themselves, their next of kin, or by a Medical Examiner. Therefore, both samples are known sex and age of modern individuals, allowing for the most reliable source of data for any forensic application.

Landmark Data

Geometric morphometric methods were used in this study. Three-dimensional landmark data records x, y, and z points on a Cartesian plane to be examined for shape and size variation. Bookstein (1991) defined three types of landmark coordinates used in recording skeletal data. Type I landmarks are those at discrete points of juxtaposed tissues, such as sutures. Type II landmarks are at a maximum geometric curvature, such as the sharpest point on a canine. Type III landmarks, also known as semi-landmarks, are

defined in respect to another feature (e.g. “most anterior”). A combination of all these types of landmarks was used to examine shape and angles in the pelvis and femur.

Landmark data were collected on the pelvis and femur using a Microscribe 3DX digitizer. This equipment uses a laser scanner to record points at the tip of the stylus, under the control of the researcher who places the end of the stylus on each landmark in succession. A total of 44 landmark and semi-landmark points were selected for the sacrum, right and left coxae, and left femur to capture the size and shape of the bone as well as the orientation of anatomical angles (Table 1.1; Figures 2.1 and 2.2).

Table 1.1: Landmarks for the os coxae and left femur

Number	Type of Landmark	Bone	Landmark	Reference
1	III	Sacrum	Midpoint of promontory	Purcell 2013
2	I	Os Coxa (right)	Posterior inferior iliac spine	Bytheway and Ross 2010
3	I		Iliac tubercle	Bytheway and Ross 2010
4	I		Anterior superior iliac spine	Bytheway and Ross 2010
5	I		Anterior inferior iliac spine	Bytheway and Ross 2010
6	III		Superior point of acetabulum	Purcell 2013
7	III		Lateral point of acetabulum	Purcell 2013
8	III		Inferior point of acetabulum	Purcell 2013
9	III		Center of acetabulum	Purcell 2013
10	III		Superiormost point of pubic symphysis	Bytheway and Ross 2010
11	III		Inferiormost point of ischial tuberosity	Bytheway and Ross 2010
12	III	Os Coxa (left)	Superiormost point on pubic symphysis	Bytheway and Ross 2010
13	III		Inferiormost point of ischial tuberosity	Bytheway and Ross 2010
14	III		Center of acetabulum	Purcell 2013
15	III		Inferior point of acetabulum	Purcell 2013
16	III		Lateral point of acetabulum	Purcell 2013
17	III		Superior point of acetabulum	Purcell 2013

Table 1.1 Continued: Landmarks for the os coxae and left femur				
18	I		Anterior inferior iliac spine	Bytheway and Ross 2010
19	I		Anterior superior iliac spine	Bytheway and Ross 2010
20	I		Iliac tubercle	Bytheway and Ross 2010
21	I		Posterior inferior iliac spine	Bytheway and Ross 2010
22	III	Femur (left)	Superiormost point on femoral head	Harmon 2009
23	III		Anteriormost point on femoral head	Harmon 2009
24	III		Posteriormost point on femoral head	Harmon 2009
25	III		Inferiormost point on femoral head	Harmon 2009
26	I		Fovea capitis	Harmon 2009
27	II		Great trochanter superior point	Harmon 2009
28	III		Superior center of neck	Purcell
29	III		Anterior center of neck	Purcell
30	I		Anterior head-neck junction	Purcell
31	III		Inferior center of neck	Purcell
32	III		Posterior center of neck	Purcell
33	II		Greater troch lateral point	Harmon 2009
34	III		Post-sup point of lesser trochanter	Harmon 2009
35	III		Midpoint of intertrochanteric line	Purcell
36	III		Posterior point of AP subtroch	Holliday et al. 2010
37	III		Medial point of ML subtroch	Holliday et al. 2010
38	III		Anterior point of AP subtroch	Holliday et al. 2010
39	III		Lateral point of ML subtroch	Holliday et al. 2010
40	I		Lateral epicondyle point	Buikstra and Ubelaker 2004
41	I		Medial epicondyle point	Buikstra and Ubelaker 2004
42	III		Posterior cruciate ligament (PCL) most medial point	Purcell
43	III		Lateral condyle point	Purcell
44	III		Medial condyle point	Purcell

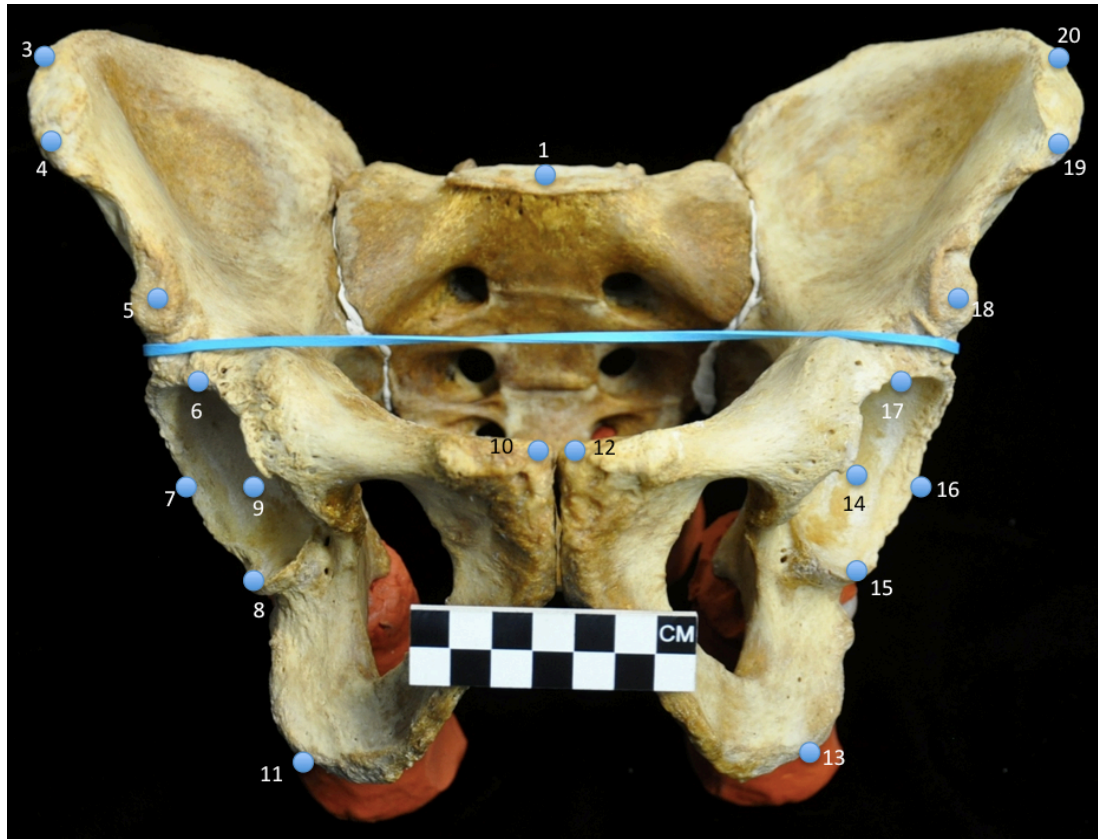


Figure 2.1: Articulated pelvis with landmarks (numbers represent landmarks described in Table 1.1)

A few landmarks required careful collection procedures. The center of the acetabulum is not well defined by most researchers, generally equating the center to be the “two right angles” within the acetabulum (Lele and Richtsmeier, 2001; Bytheway et al., 2010). The acetabulum is not a perfect spherical shape; it is more elliptical. Furthermore, the complex three-dimensional shape of the os coxa makes consistent orientation of the bone necessary when collecting data. To obtain the acetabular center, for the purposes of this study, a large rubber band was placed around the middle of the pubic symphysis and stretched to the most lateral point on the acetabulum. This lateral point formed Landmarks 7 (right side) and 16 (left side), and bisecting this line provided the superior and inferior points on the acetabulum (Figure 2.3).

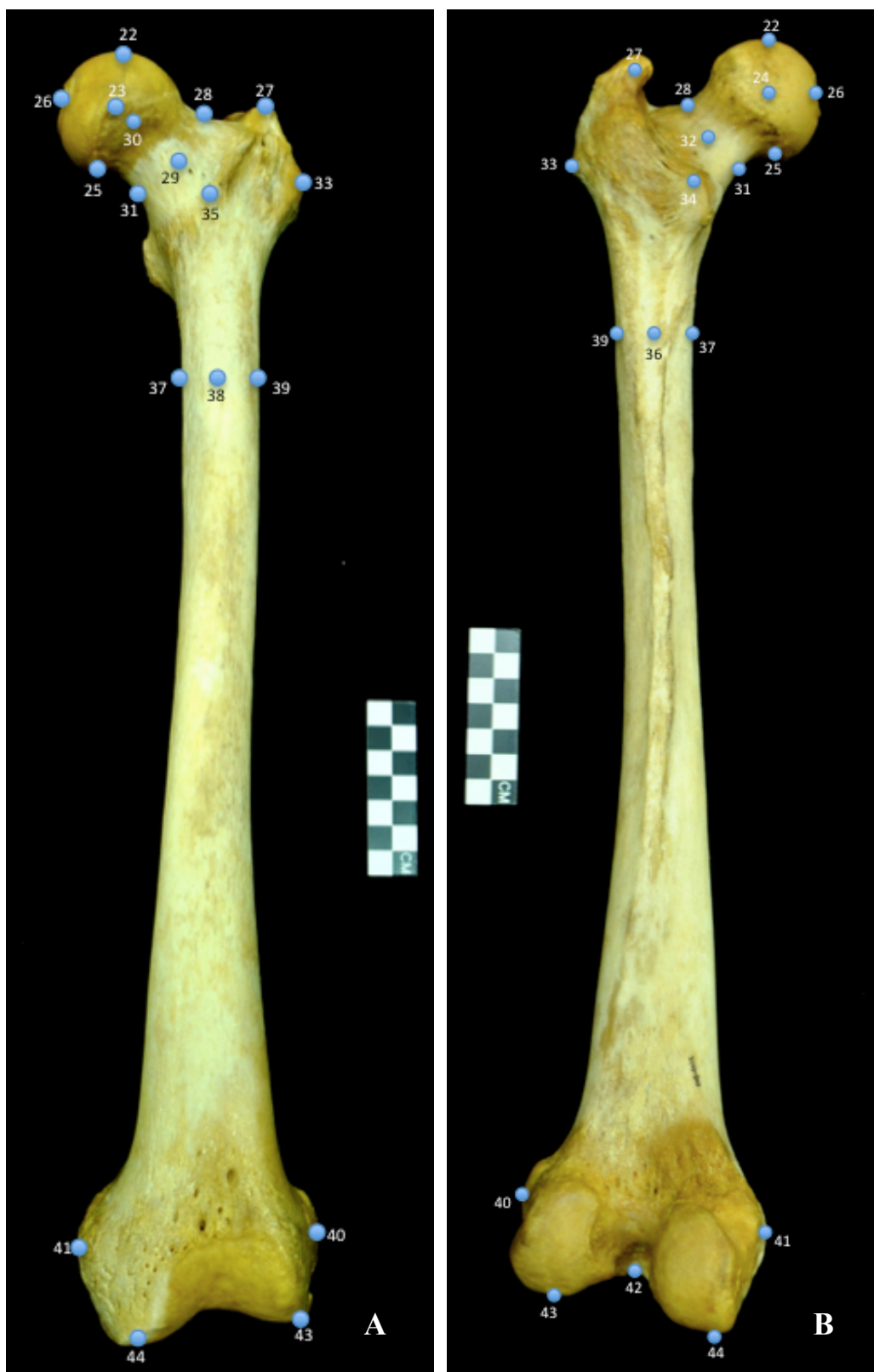


Figure 2.2: Anterior (A) and posterior (B) views of femur with landmarks (numbers represent landmarks defined in Table 1.1)



Figure 2.3: Acetabulum measurements for landmarks 14-17 on the left os coxa (landmarks 6-9 on right side)

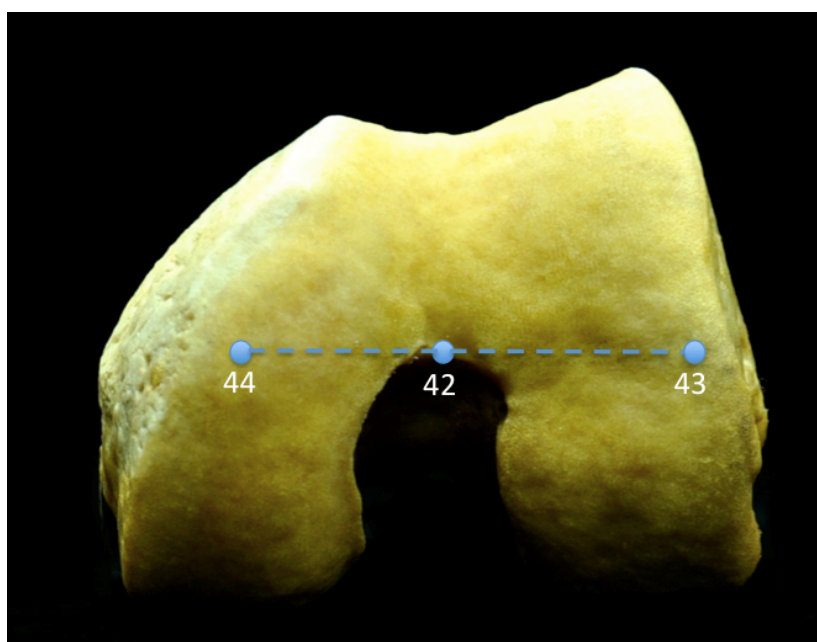


Figure 2.4: Femoral condyle measurements (numbers represent landmarks defined in Table 1.1)

The two femur condyle points (Landmarks 43 and 44) were collected so that the points were parallel to the transverse plane when the femur was placed flat on the table, anterior side up (Figure 2.4). This allowed for collection of the femoral version angle. The area on each condyle along that parallel line that would articulate with the tibia formed Landmarks 43 and 44.

All semi-landmarks were marked with a pencil before the bones were placed on the clay pillars for data collection. For the pelvis, the three bones were articulated with rubber bands and sticky-tac® in the sacro-iliac joint (Figure 1.1). The bones were then secured on three clay pillars for digitizing. The pelvis landmarks provide information about the overall shape of the pelvis, as well as bi-iliac breadth and biacetabular breadth.

For the femur, two clay pillars rested under the femur: one between the proximal end and midpoint, one between the distal end and the midpoint (Figure 2.5). These landmarks provided information about the size and shape of the femoral head and neck, cross-sectional dimensions of the diaphysis at subtrochanteric and midshaft, and the position of the medial and lateral condyles. All data were recorded onto an Excel ® file



Figure 2.5: Femur on clay pillars for landmark data collection

or with the 3Skull software developed by Steve Ousley and later exported to Excel ® for analysis.

Calculation of Measurements and Angles from 3D Coordinate Data

When examining shape differences, such as variation in femur angles, it is important to consider the total morphology of the femur. Biacetabular breadth, bi-iliac breadth, neck length, biomechanical neck length and anatomical length provide a more accurate understanding of the biomechanical influences on femur shape. The femoral bicondylar and neck-shaft angles work to align the knees with the body's center of mass. Therefore, two individuals with the same bicondylar breadth could display different neck-shaft angles because one individual has a shorter femoral neck or longer femur length. Table 1.2 summarizes the metric measurements for the femur and os coxae, with corresponding photo illustration in Figures 2.6 and 2.7.

Inter-landmarks distances provided neck length, anatomical length, biomechanical neck length, biacetabular breadth, and bi-iliac breadth. The following standard distance formula was used to find the length between two points (X_1, Y_1, Z_1) and (X_2, Y_2, Z_2) :

$$\sqrt{(X_1 - X_2)^2 + (Y_1 - Y_2)^2 + (Z_1 - Z_2)^2}$$

These lengths were then analyzed with a one-way ANOVA in the Statistical Product and Service Solutions (SPSS®) software to estimate the variation using sex as the independent variable to test for sexual dimorphism. These calculations provided size variation to later compare with shape data.

Table 1.2: Metric measurements of the os coxae and femur

Bone	Measurement	Definition	Reference
Ox Coxae	Biacetabular breadth	Distance between the middle of the acetabulae (Landmarks 9 and 14)	Tague 1989
	Biliac breadth	Distance between the iliac tubercles in the os coxae (Landmarks 3 and 20)	Tague 1989
Femur	Neck length	Distance between the anterior head-neck junction and the intertrochanteric midpoint line (Landmarks 30 and 35)	Harmon 2009
	Biomechanical neck length	Distance between the superiormost point of the head to the most lateral point of the greater trochanter (Landmarks 22 and 33)	Harmon 2009
	Epicondylar breadth (<i>for shape analysis only</i>)	Distance between the two most laterally projecting points of the epicondyle (Landmarks 40 and 41)	Buikstra and Ubelaker 1994
	Anatomical length	Superior point on head to medial condyle point (Landmarks 22 and 44)	Purcell

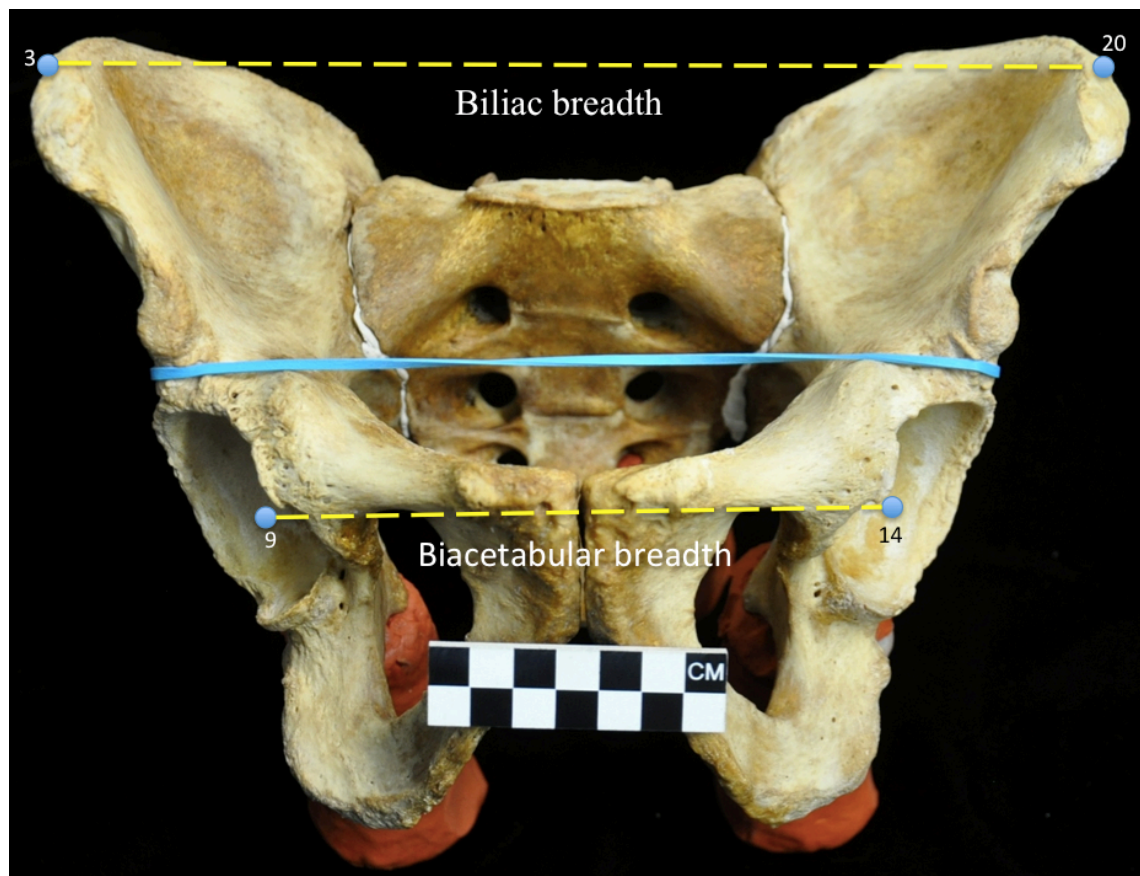


Figure 2.6: Metric measurements of the pelvis (landmarks correspond to those in Table 1.2)

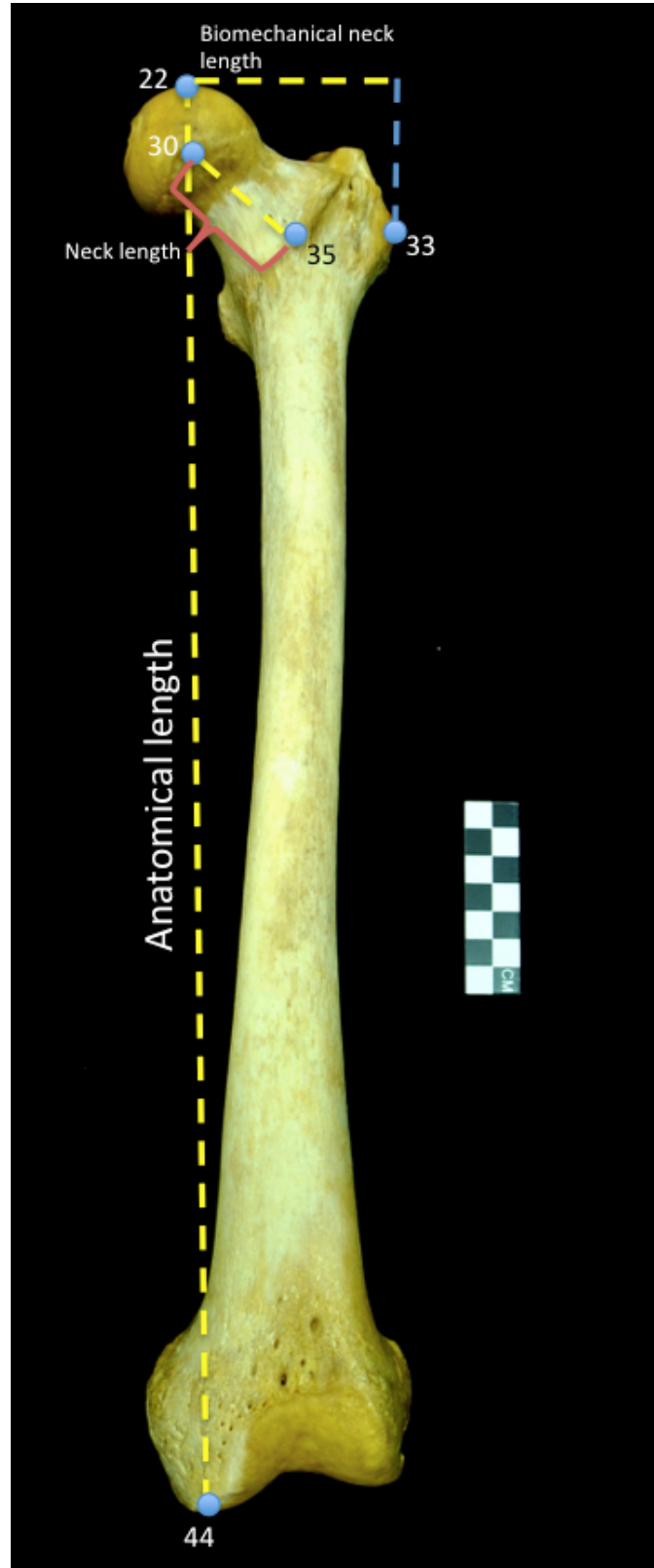


Figure 2.7: Metric measurements of the femur with corresponding landmarks

Angles included for measurement in the femur include: neck-shaft angle, bicondylar angle, and femoral angle of version. The collected landmarks provided the necessary axes for these angles (Table 1.3 and 1.4, Figures 2.8-2.10). Vector analysis provided the necessary information to obtain the angles. A vector is a line with a specific magnitude (length) and direction. The collected landmarks provided the coordinate points with which to calculate a vector. The intersection of the two vectors/axes formed the angle, also known as a dot product of two vectors. Table 1.3 details which landmarks were utilized for each axis.

First, it is necessary to define the axes and landmarks points in terms of vectors. The two axes used to calculate the angle will be defined as vectors P and Q . The vectors are the x, y and z components of the two landmark points in each axis. For example, in Figure 2.8, the subtrochanteric center (STC) and Landmark 42 are the two points that form the femoral longitudinal axis/vector (FLA), while Landmarks 43 and 44 form the femoral condyle transverse functional axis/vector (FCT). The following formula provides the x, y, and z components for the vectors:

$$P = (X_1 - X_2); (Y_1 - Y_2); (Z_1 - Z_2)$$

$$Q = (X_1 - X_2); (Y_1 - Y_2); (Z_1 - Z_2)$$

Then, the product of these components was added for each vector and divided by the product of the magnitude (lengths) of the two vectors to provide the scalar product and angle in radians:

$$\cos \theta = \frac{P_x Q_x + P_y Q_y + P_z Q_z}{PQ}$$

The product of the θ and 57.3 converts the angle unit degrees (1 radian = 57.3 degrees).

Table 1.3: Derived point and axes

Measurement/axis	Definition	How is it used?	Reference
Femoral head center (FHC)	Midpoint of landmarks 23 and 24	Neck-shaft angle	Harmon 2009 (modified)
Femoral neck center (FNC)	Midpoint of landmarks 29 and 32	Neck-shaft angle	Harmon 2009 (modified)
Subtrochanteric center (STC)	Midpoint of landmarks 37 and 39	Femoral longitudinal axis	Yoshioka et al. 1987 (modified for morphometrics)
Femoral longitudinal axis (FLA)	Subtrochanteric center (Landmarks 37 and 39) to the posterior cruciate ligament attachment (landmark 42)	Bicondylar angle	Yoshioka et al. 1987; Heiple and Lovejoy 1971
Femoral condyle transverse functional axis (FCT)	Landmarks 43 and 44	Femoral angle of version	Yoshioka et al. 1987
Acetabular center (Landmarks 9 and 14)	Intersection of landmarks 6, 7, and 8 for the right os coxa; 15, 17 and 17 for left os coxa	Biacetabular breadth	Purcell
Femoral neck axis (FNA)	FHC to FNC	Neck-shaft angle and femoral angle of version	Harmon 2009 (modified)

Table 1.4: Angle measurements

Angle	Definition	Reference
Bicondylar/oblique angle (Figure 2.11)	Angle of the FCT (Landmarks 43 and 44), to the FLA (Landmarks 37 and 39)	Yoshioka et al. 1987 (modified)
Femoral angle of version (Figure 2.10)	The FNA (Landmarks 23, 24; 29, 32) intersecting with the FCT (Landmarks 43 and 44)	Yoshioka et al. 1987 (modified)
Neck-shaft angle (Figure 2.9)	Center of femoral head (Landmarks 23 and 24) through the center of the neck (Landmarks 29 and 32), intersecting with the femoral longitudinal axis (Landmarks 37, 39 and 42)	Yoshioka et al. 1987 (modified)

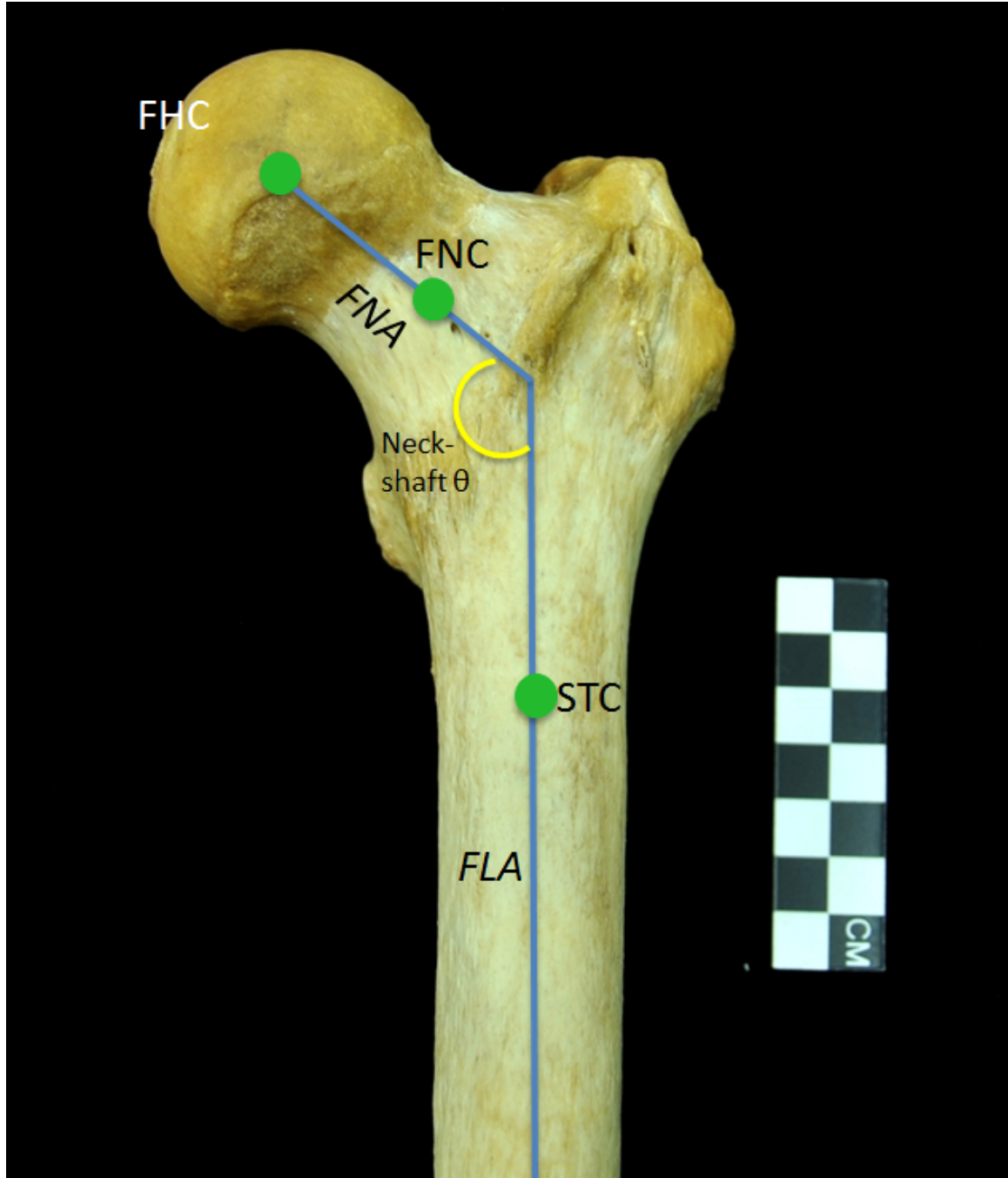


Figure 2.8: Neck-shaft angle of the femur, anterior view (corresponding to derived points and axes, and angles in Tables 1.3 and 1.4)

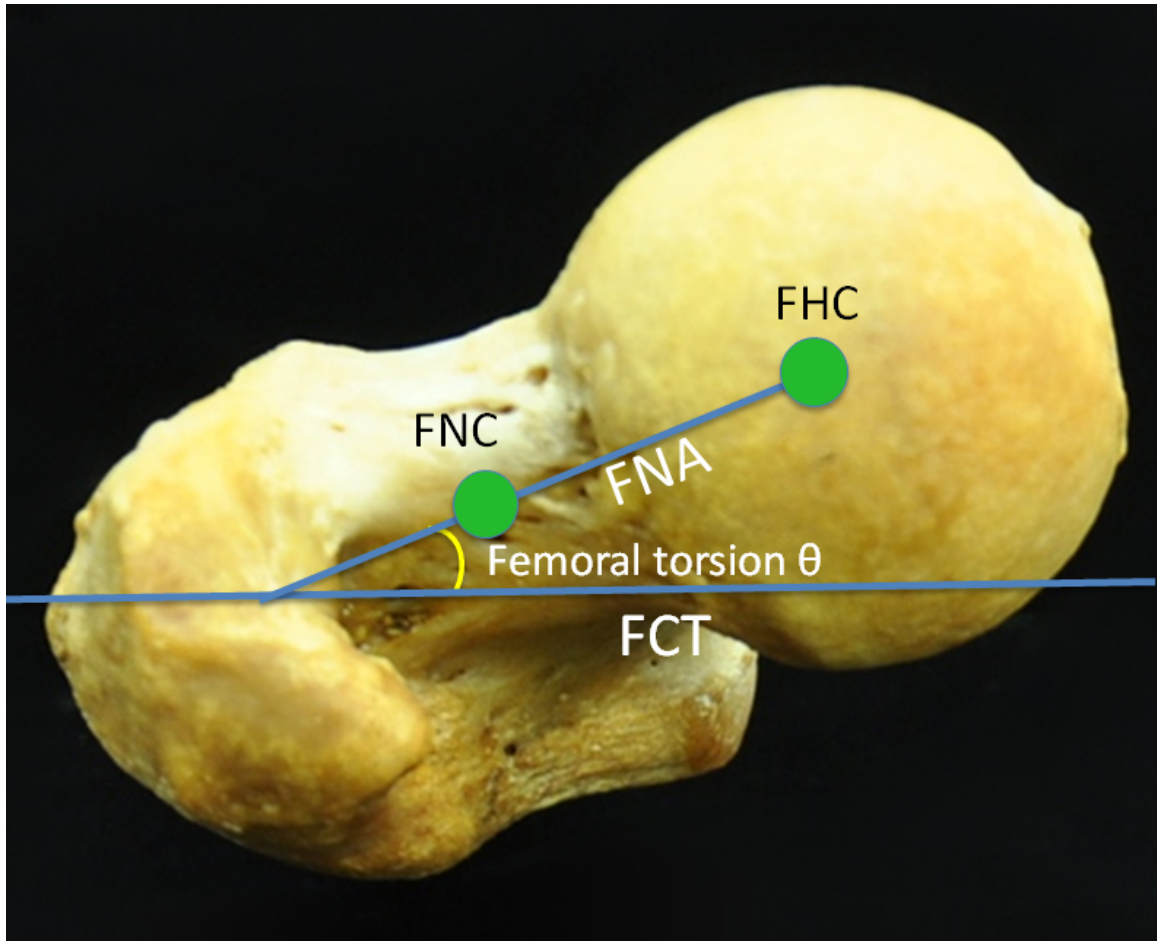


Figure 2.9: Femoral version angle/torsion, superior view, anterior is up (corresponding to derived points and axes, and angles in Tables 1.3 and 1.4)



Figure 2.10: Bicondylar/oblique angle of the femur, anterior view (corresponding points and axes, and angles in Tables 1.3 and 1.4)

The femoral bicondylar angle is measured directly from the bone, and will therefore be within a 80-90 degree range rather than a 5-15 degree range as is observed in some other studies that measured the angle as perpendicular to the infracondylar plane.

A one-way ANOVA in SPSS software was used to test for significant sexual dimorphism in neck-shaft angle, femoral version angle and bicondylar angle. A linear regression model examined the relationship between these angles and the length measurements in the pelvis and femur. A discriminant function analysis (DFA) in SPSS was used to evaluate the effectiveness of the femur at estimating sex. A stepwise procedure was used for variable selection among the variables of femoral angle and neck lengths in the DFA. This procedure selects a subset of variables based on the squared partial correlation and the significant level from an analysis of covariance that has the greatest amount of discriminating ability.

Analysis of the 3D Data

The coordinates of each landmark were imported into the 3D morphometric software, MorphoJ (Klingenberg 2008) to visualize differences between males and females in the size and shape of the bones and the position of major muscle attachment sites. Coordinate data were arranged into a common coordinate system using a Generalized Procrustes Analysis (GPA). The software MorphoJ uses Procrustes superimposition to project the data into tangent space using orthogonal projection. This method of superimposition is a least-squares method that uses orthogonal projection to reduce non-shape variation. First, the centroid (center of object) of each individual's

landmark data set is calculated to center the landmarks to a common centroid. The landmarks are then rotated and scaled until the sum of squared distances to corresponding landmarks is minimized. This is to remove non-shape variation. In other words, each sample is scaled larger or smaller to be most alike in size, therefore size is removed as a variable.

A “find outliers” procedure in MorphoJ was used to check for intraobserver error within the data set. A Procrustes analysis of variance (ANOVA) for shape analyzed the sex-based variation of the landmarks in both the femur and pelvis. To examine the most significant differences in shape between males and females, a covariance matrix pooled by sex was created, and a Principle Component Analysis (PCA) was performed. These changes are represented visually with wireframe graphs and PC scatterplots. This was also the method utilized to visually assess acetabular version. Currently accepted methods available for comparison are radiographic and MRI techniques (Stem et al., 2006), and it is unclear if variations in pelvic tilt and overall body composition may affect the efficacy in using these techniques as a comparison to dry bone measurement. Therefore, a wireframe graphical representation of the PCA changes between males and females provides a visual assessment of this variable.

Discriminate function analysis (DFA), a procedure that maximizes within-group differences, was utilized with the Procrustes data points. Evaluation of the discriminating ability of the variables selected was then assessed using a cross-validation procedure. The cross-validation procedure evaluates the predictive power of the statistical model.

CHAPTER III

RESULTS

Analysis of Lengths and Angles

A Shapiro-Wilk test of normality was used to examine if the calculated angles and lengths were from a normally distributed population. The null hypothesis is that the variables are normally distributed, and a p-value of <0.05 rejects the null hypothesis. Two outliers were found and removed from the neck-shaft angle variable set, and one from the biacetabular breadth set. After the outliers were removed, these variables displayed a normal distribution. All other variables except for femoral version (torsion angle) were normally distributed (Table 2.1).

Table 2.1: Tests of normality in the pelvis and femur

Measurement	Shapiro-Wilk P-Values
Neck-Shaft Angle (with two outliers)	.037
Neck-Shaft Angle (outliers removed)	.058
Bicondylar Angle	.812
Anatomical Length	.945
Neck length	.961
Femoral Torsion Angle	.000
Biomechanical Neck Length	.050
Bi-iliac Breadth	.349
Biacetabular breadth (one outlier)	.914
Biacetabular breadth (outlier removed)	.029

A one-way ANOVA was used to examine sexual dimorphism in the size of the biacetabular breadth (H_{01}), bi-iliac breadth (H_{02}), biomechanical neck length (H_{03}), neck-shaft angle (H_{06}), and bicondylar angle (H_{07}). Bi-iliac breadth did not exhibit significant

size sexual dimorphism, but biacetabular breadth, biomechanical neck length, and the two angles differed significantly (Table 2.2; Figures 3.1-3.4). Females have a wider biacetabular breadth and greater neck angle, but biomechanical neck length and smaller bicondylar angles than males. A nonparametric test (Mann-Whitney U) was used to analyze sexual dimorphism of femoral version (H_04), with a significant p-value of 0.003 (Table 2.12). Overall, females display a larger femoral angle of version than males.

Table 2.2: Tests of sexual dimorphism in measurements and angles

Measurement	P-Value ¹
Biacetabular breadth ²	0.004
Bi-iliac Breadth ²	0.206
Biomechanical Neck Length ²	<.001
Neck-Shaft Angle ²	0.041
Femoral Bicondylar Angle ²	<0.001
Femoral Version ³	0.003

¹ null hypothesis of no sexual dimorphism is rejected at $p \leq 0.05$

²ANOVA

³Mann-Whitney U test

The Pearson correlation test examined H_010 - H_012 (Table 2.3). Additional correlation tests were performed on all normally distributed significant variables to better understand the variability and uncover other possible significant relationships in the data. The “Cubed Root” Variable is the cube root of the product of biacetabular breadth, neck length, and anatomical length. Regressed against the bicondylar and neck-shaft angles, it would demonstrate the effect of size differences on these angles (Dorrach and Mosimann, 1985).

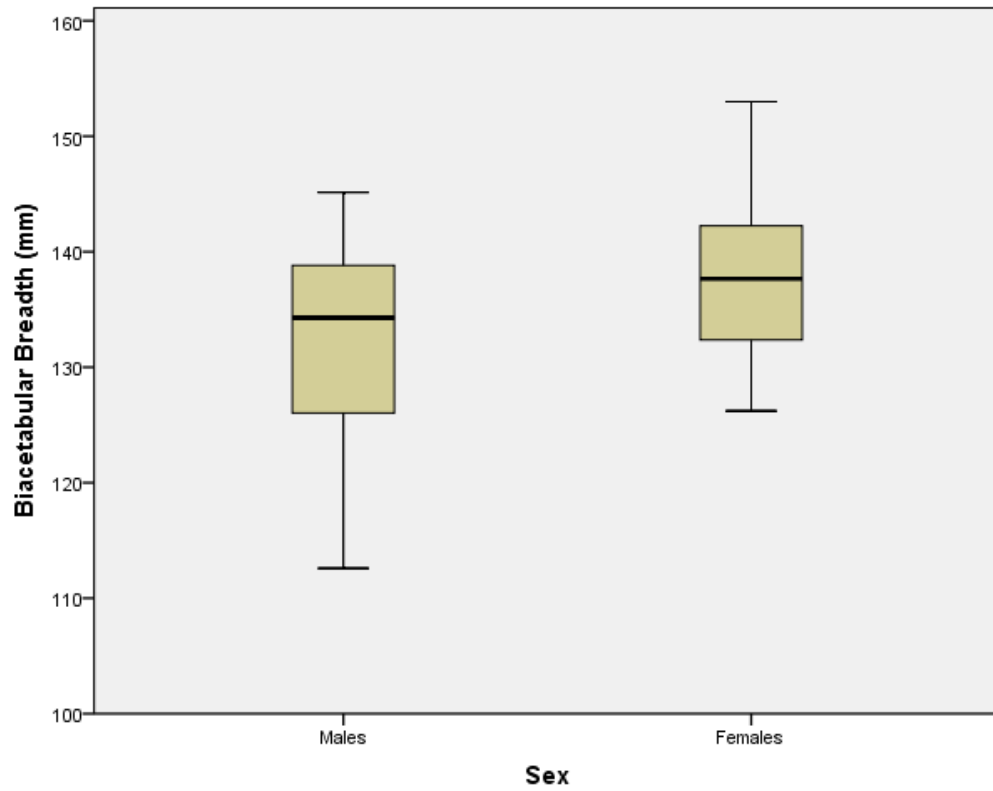


Figure 3.1: Distribution of male and female biacetabular breadth

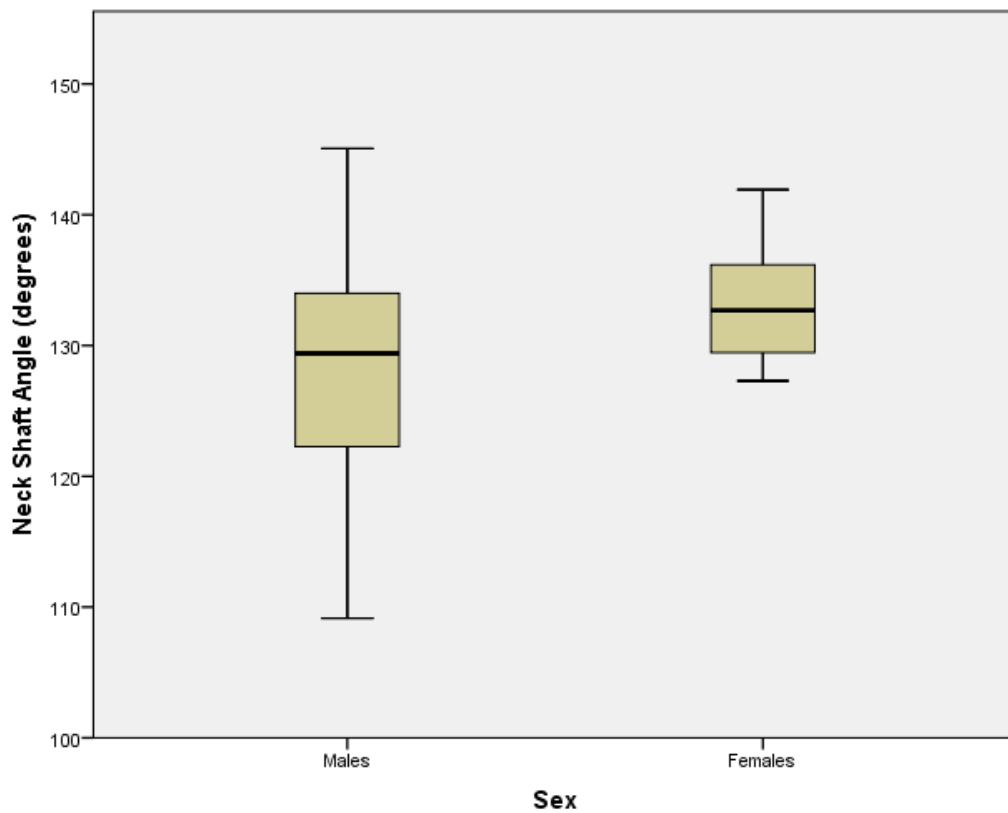


Figure 3.2: Distribution of male and female neck-shaft angle

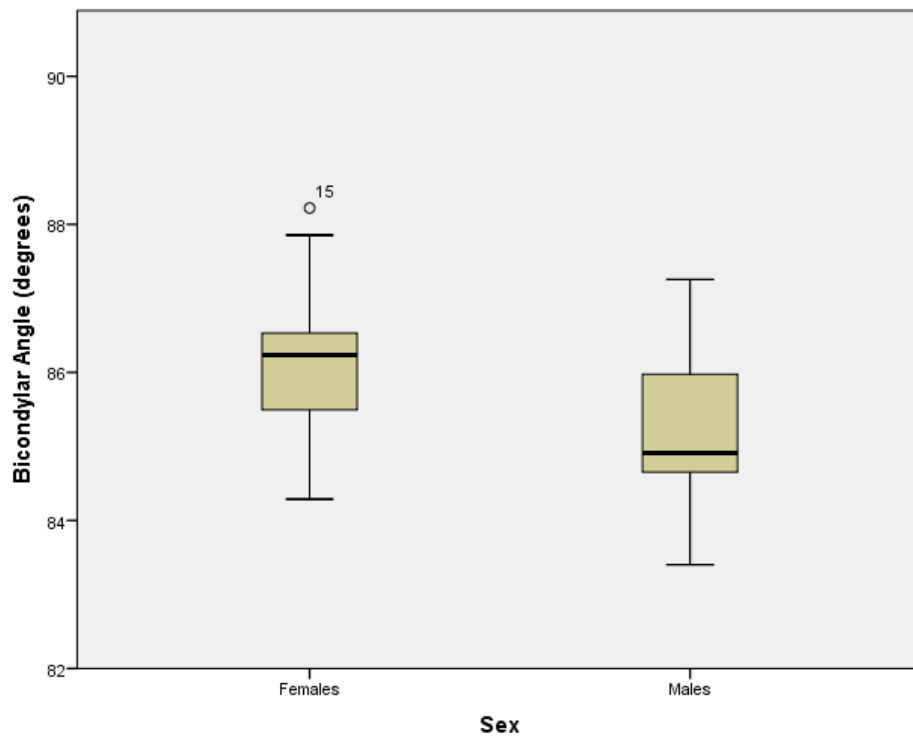


Figure 3.3: Distribution of male and female bicondylar angle

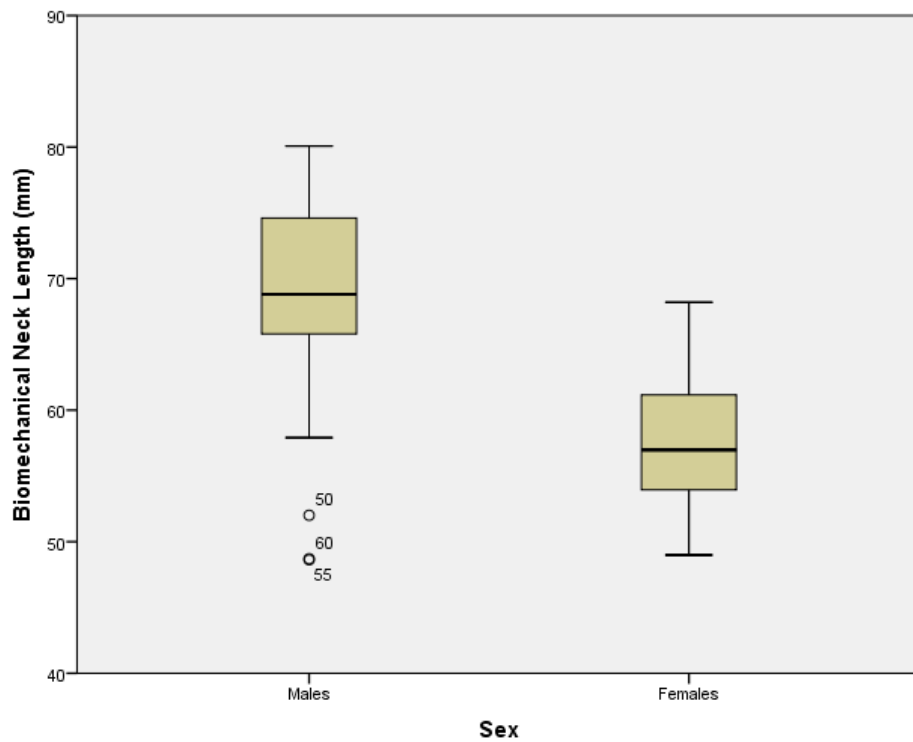


Figure 3.4: Distribution of male and female biomechanical neck length

Table 2.3: Pearson correlation table for pelvic and femoral measurements¹

	Biacetabular breadth	Bicondylar angle	Neck-shaft angle	Biomechanical neck length	Cubed Root
Biacetabular breadth	1	0.340	0.384	-0.198	N/A
Bicondylar angle	0.340	1	0.667	-0.517	0.101
Neck-shaft angle	0.384	0.667	1	-0.468	0.065
Biomechanical neck length	-0.198	-0.517	-0.468	1	
Cubed Root	N/A	0.101	0.065	N/A	1

¹ *Bold correlations are significant (2-tailed)*

All significant correlations were then graphed as linear regression equations, with separate regression lines for males (black) and females (gray) to detect sex variation in correlations (Figure 3.5-3.10). There is a weak relationship between bicondylar breadth and biacetabular breadth among males, but a moderate relationship in females. However, a positive relationship between neck-shaft angle and biacetabular breadth exists for both sexes. The bicondylar angle and neck-shaft angle also indicate a very significant positive relationship for both sexes. But a negative relationship exists between the two angles and biomechanical neck length, meaning that the longer the lever arm for the femur, the smaller the femoral angle. The cubed root variable was not significant for any of the angles, indicating that size was not a significant variable in determining angle degree.

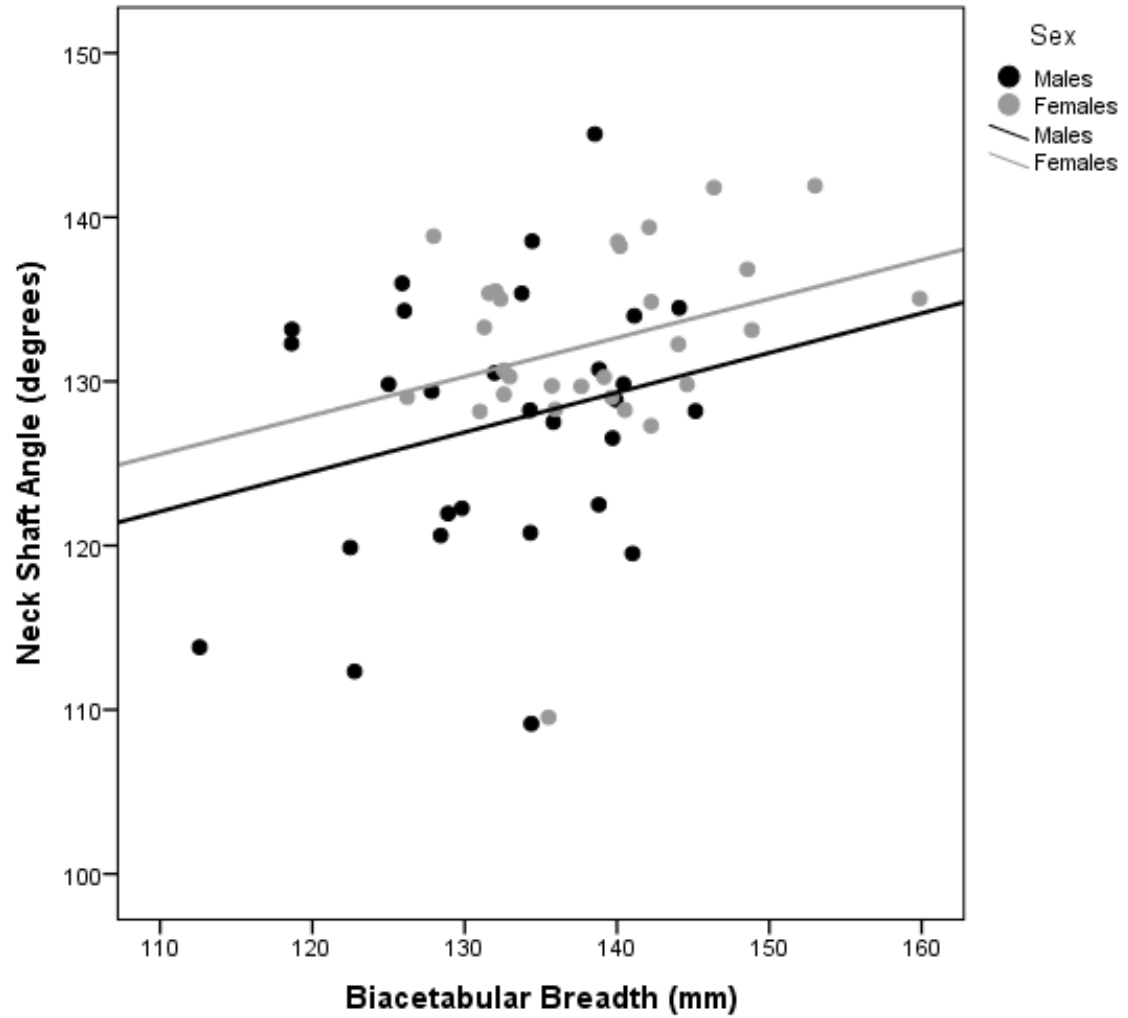


Figure 3.5: Regression of neck-shaft angle (degrees) and biacetabular breadth (mm)

R^2 values: Males 0.061; Females 0.088

*Equations: Males $y=99.54+0.24*x$; Females $y=95.51+.24*x$*

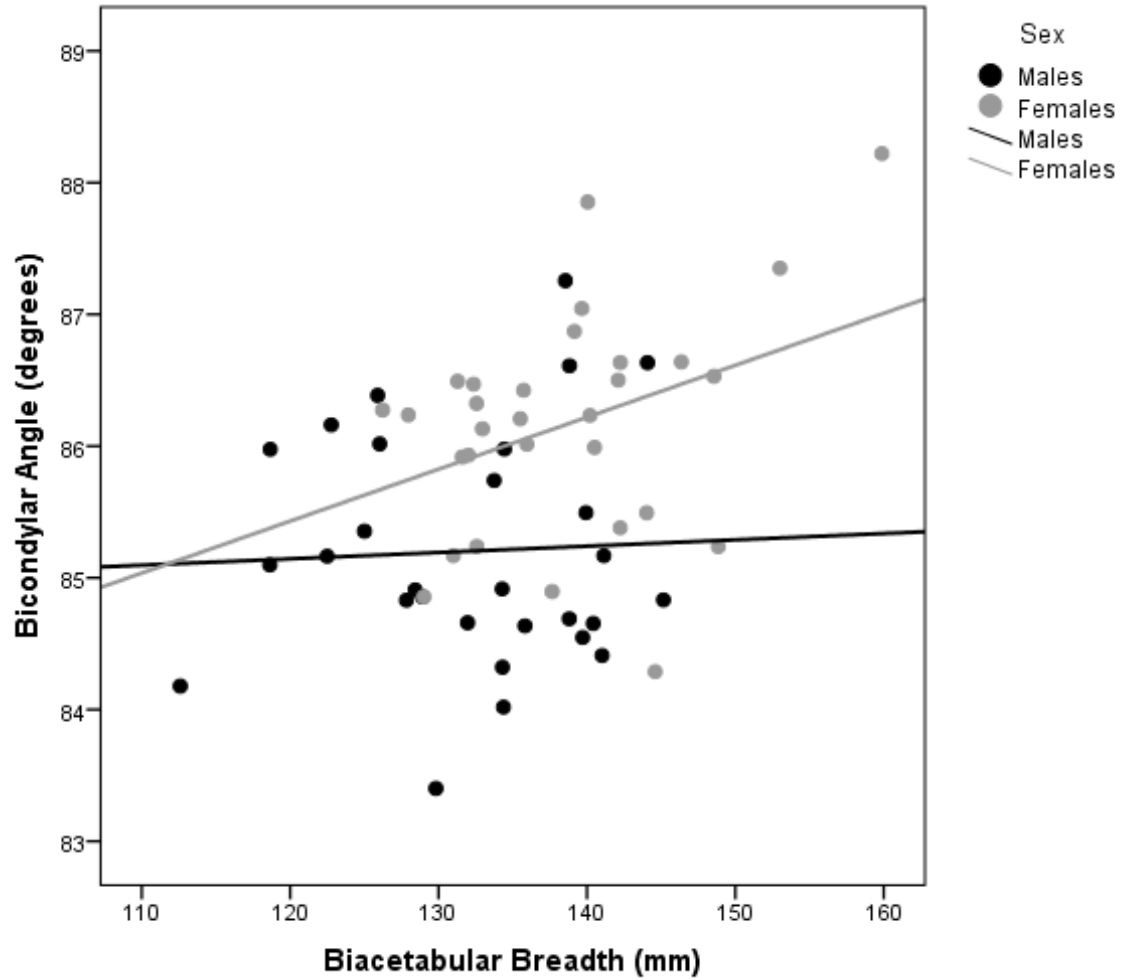


Figure 3.6: Regression of bicondylar angle (degrees) and biacetabular breadth (mm)

R^2 values: Males 0.002; Females 0.128

*Equations: Males $y=84.57+0.0048*x$; Females $y=80.7+0.04*x$*

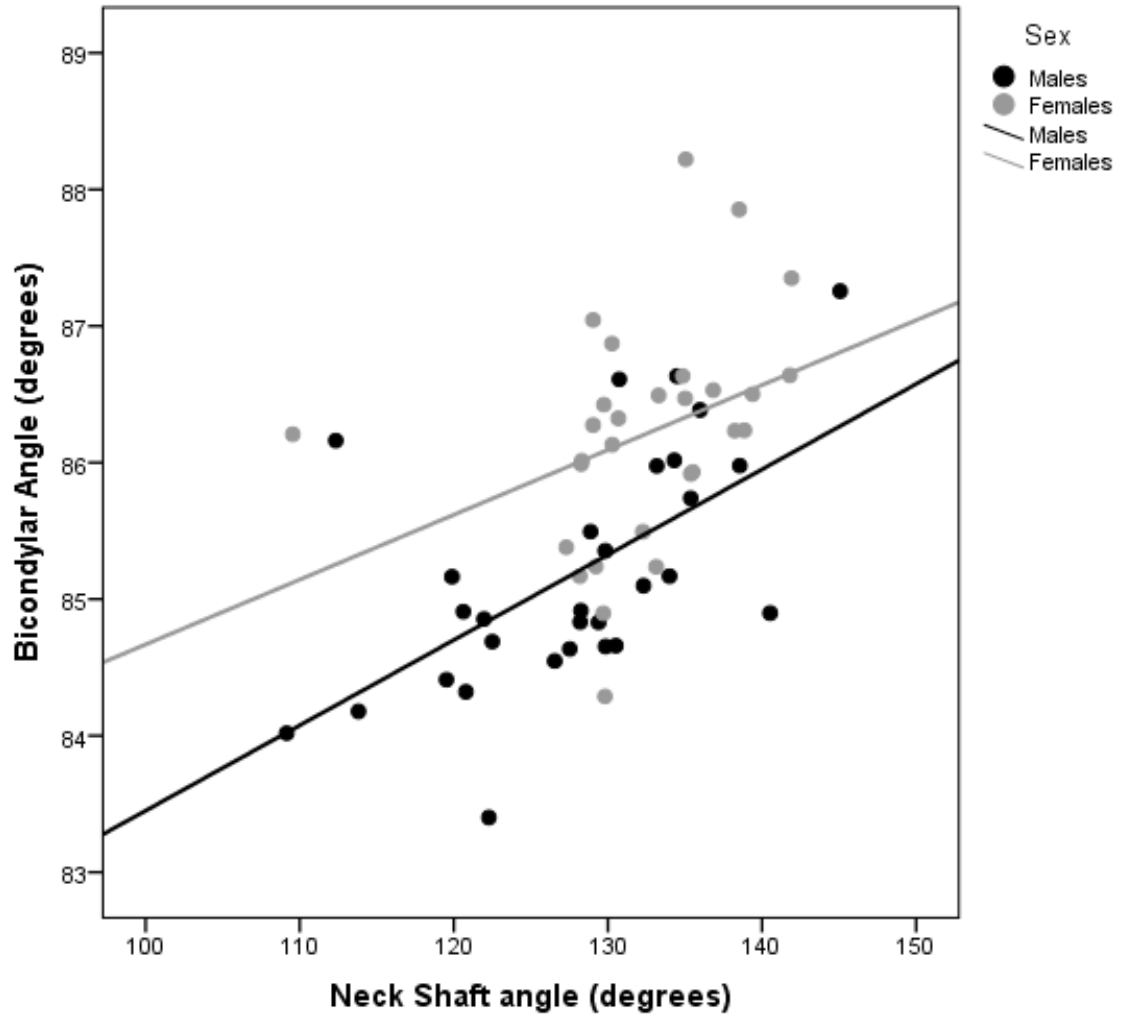


Figure 3.7: Regression of neck shaft angle (degrees) and bicondylar angle (degrees)

R^2 values: Males 0.354; Females 0.121

*Equations: Males $y=77.2+0.06*x$; Females $y=79.92+0.05*x$*

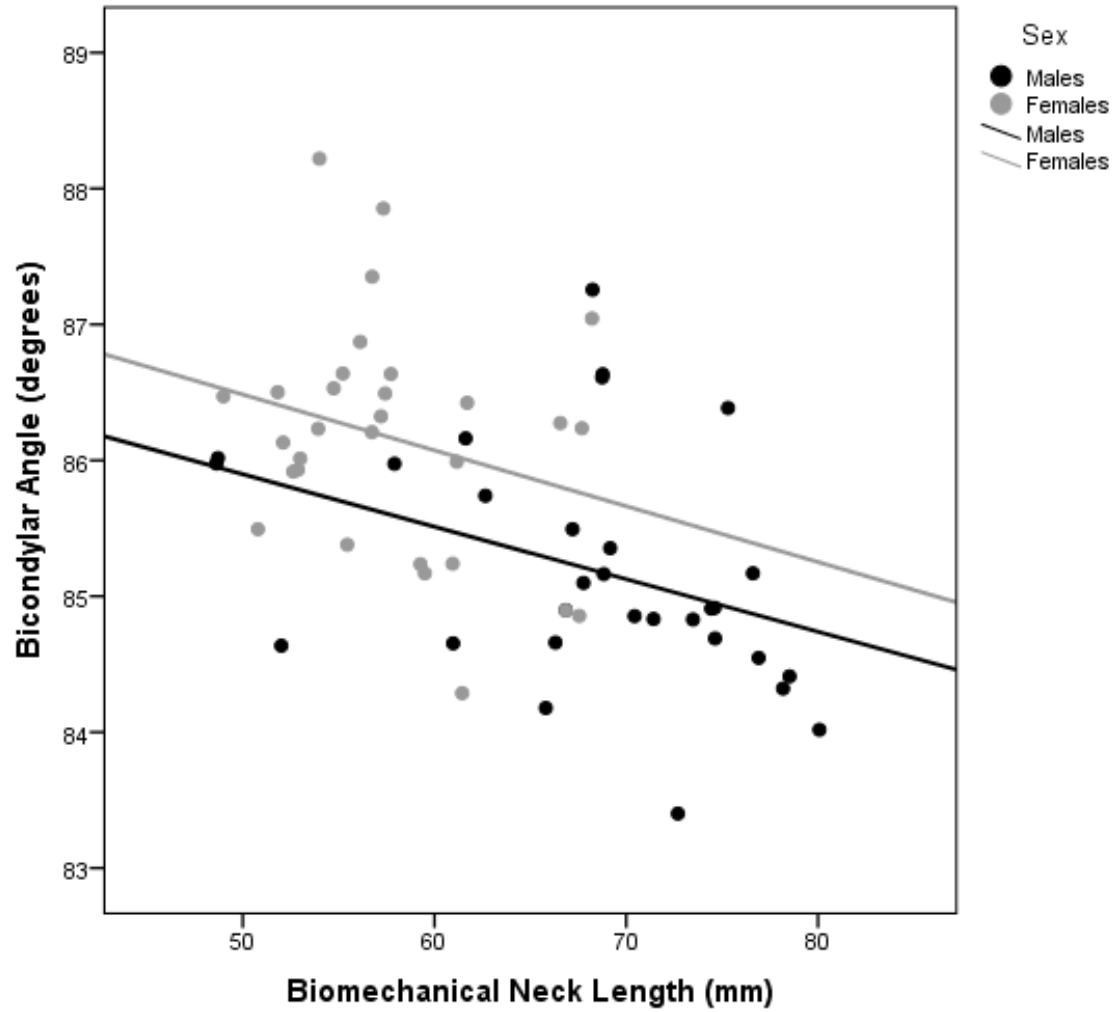


Figure 3.8: Regression of bicondylar angle (degrees) and biomechanical neck length (mm)

R^2 values: Males 0.135; Females 0.066

*Equations: Males $y=88.54+-0.04*x$; Females $y=87.83+-0.04*x$*

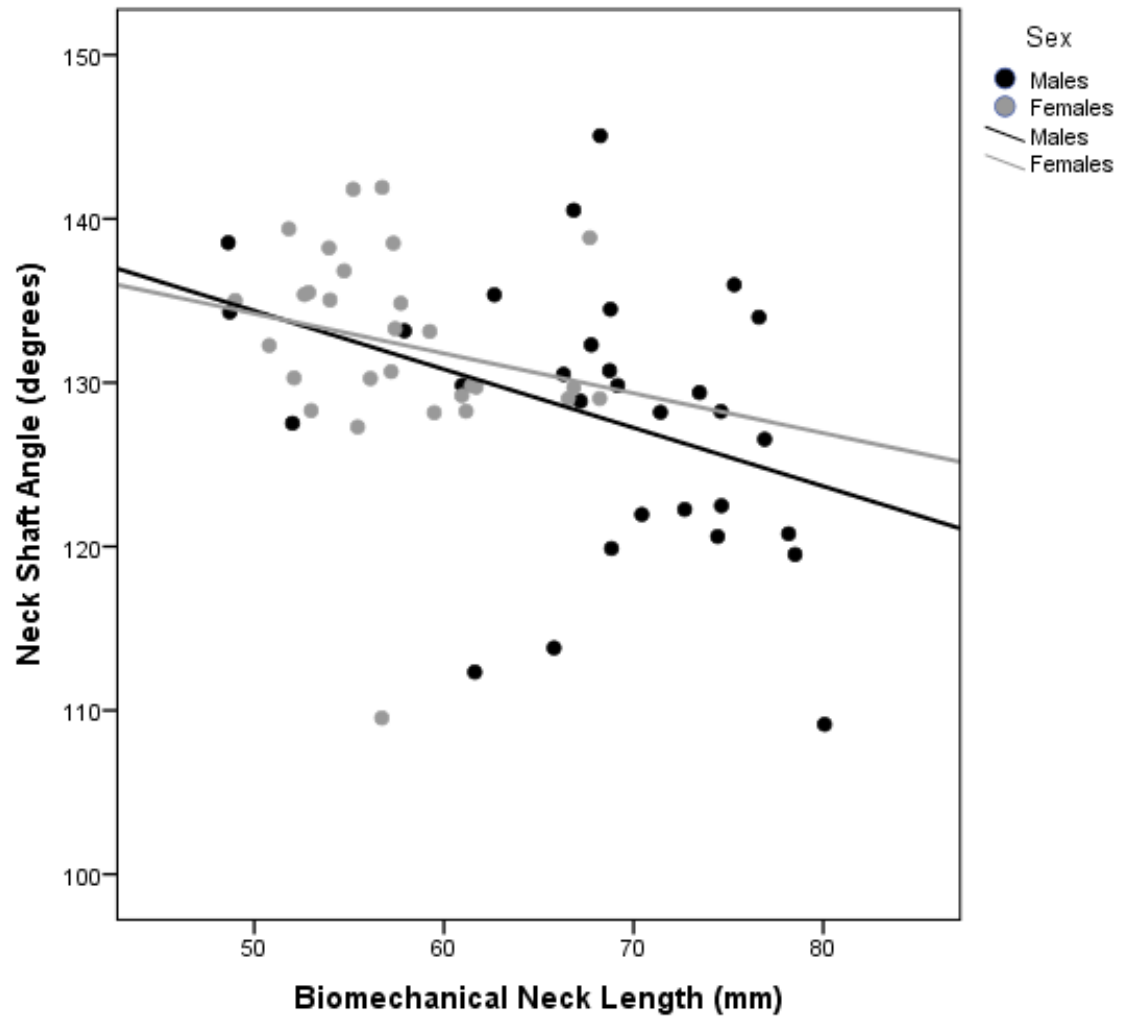


Figure 3.9: Regression of neck-shaft angle and biomechanical neck length

R^2 values: Males 0.127; Females 0.041

*Equations: Males $y=146+-0.24*x$; Females $y=152+-0.36*x$*

Analysis of Landmark Data

The software program MorphoJ was used to perform the Procrustes fit and ANOVA for the pelvic and femoral landmark data to test H_{05} , H_{08} , and H_{09} . The shape ANOVA between the male and female groups had a p-value of $<.0001$ for the pelvis and femur, meaning that the shape-only differences in the landmarks of the two groups were statistically significant. The discriminate function analysis (DFA) and cross-validation procedure examined how well the landmarks estimated the variation (Tables 2.4 and 2.5). The DFA table results examine how the landmark shape variation differs between males and females, and how well each sample belongs in its respective group (if it is allocated to that group). A cross-validation procedure tests the ability for the 3D coordinates to correctly allocate a bone to the male or female group (i.e. estimate sex). The DFA shows that the landmark points on both the pelvis and femur display enough variation to count males and females as two distinct groups. The CVA allocates most of the individuals to their correct sex with the pelvis, but the femur correctly allocates only about 2/3 of individuals.

Figures 3.10-3.15 are wireframe graphs of the vectors for the landmark changes between males and females (PC1 and PC2 respectively). The light gray represents the mean shape, while the black represents the most significant shape variation between males and females. The head and neck positions are the most consistently different between males and females for both the PC1 and PC2 graphs for the femur (Figures 3.10 and 3.11), suggesting a difference in the overall neck-shaft angle. Finally, the distal femur points in Figure 3.11 show a variation for a narrower epicondylar breadth relative to the femoral shaft, and a shift in condylar articulation points.

Figures 3.12 – 3.15 display the changes in the os coxae, first from an anterior view (Figures 3.12 and 3.13), and then from a superior view (Figures 3.14. and 3.15).

The iliac blades in Figure 3.12 are significantly more flared for the female group.

Additionally, the acetabulum vectors in Figure 3.14 display more anteverted acetabula for females than for males. The graphs of the PCA in Figure 3.16 shows overlap in the two samples for the femur, while the PCA in Figure 3.17 displays a fairly distinct separation for PCA in the pelvis.

Table 2.4: DFA for pelvis and femur

Bone	Group	Female	Male	Total
<i>Pelvis</i>	Female	30	0	30
	Male	0	30	30
<i>Femur</i>	Female	30	0	30
	Male	0	30	30

Table 2.5: CVA for pelvis and femur

Bone	Group	Female	Male	Total
<i>Pelvis</i>	Female	25	5	30
	Male	5	25	30
<i>Femur</i>	Female	21	9	30
	Male	11	19	30



Figure 3.10: PC1 of Landmark differences between females and males in the femur (Landmark numbers correspond to those in Table 1.1)



Figure 3.11: PC2 of Landmark differences between females and males in the femur (Landmark numbers correspond to those in Table 1.1)

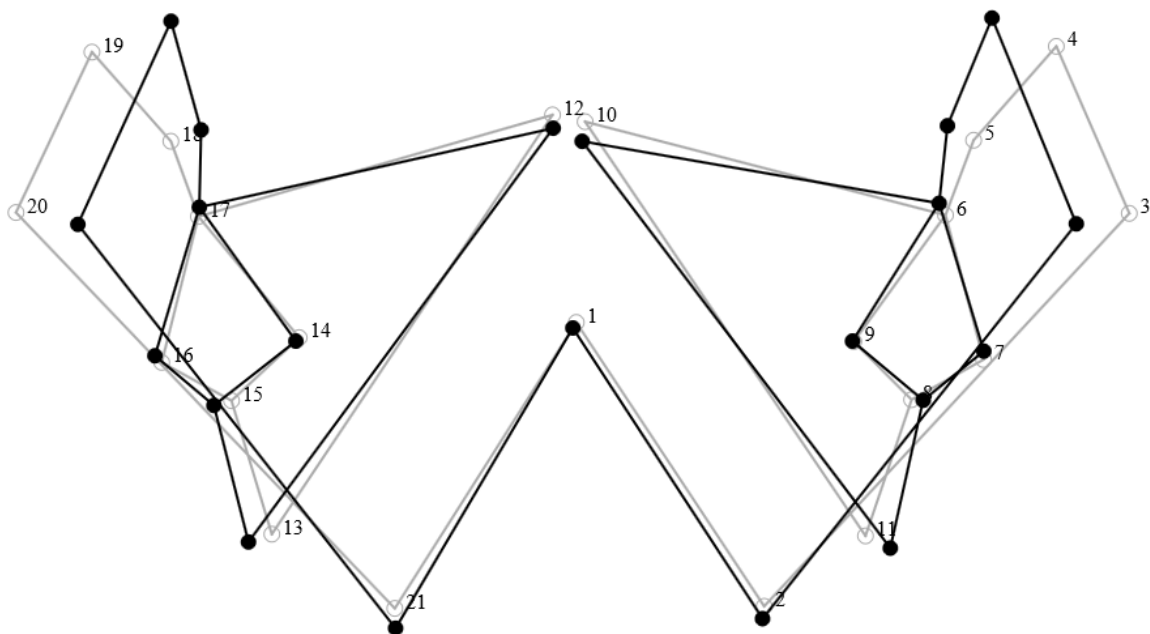


Figure 3.12: PC1 shape differences between females and males in the pelvis in the anterior view (Landmark numbers correspond to those in Table 1.1)

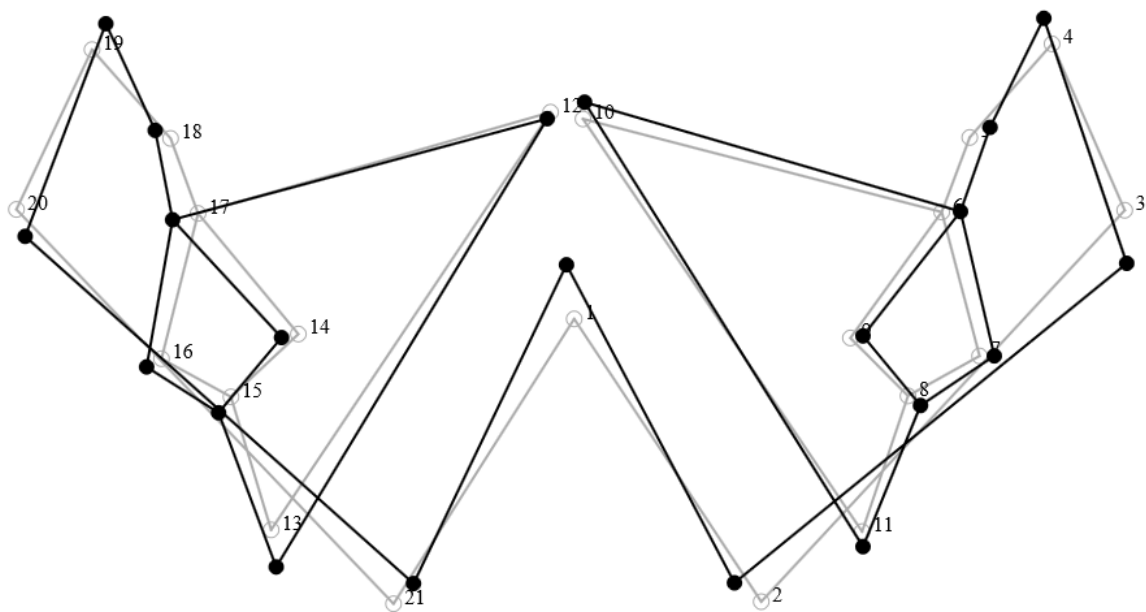


Figure 3.13: PC2 shape differences between females and males in the pelvis in the anterior view (Landmark numbers correspond to those in Table 1.1)

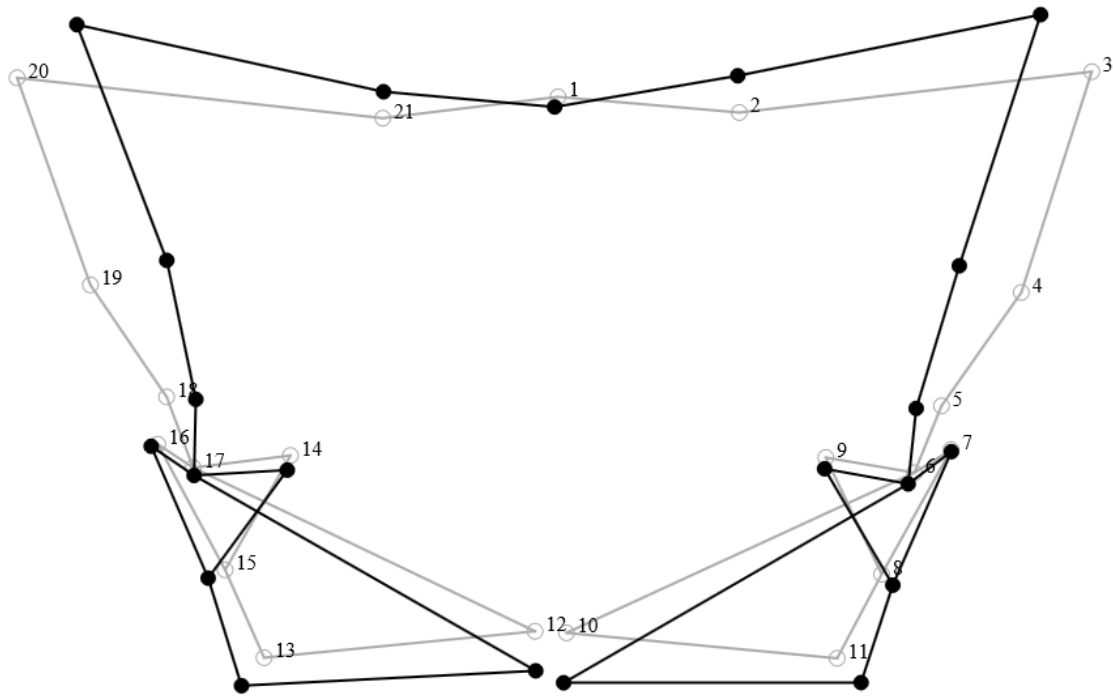


Figure 3.14: PC1 shape changes between females and males in the pelvis in the superior view, posterior is up (landmark numbers correspond to those in Table 1.1)

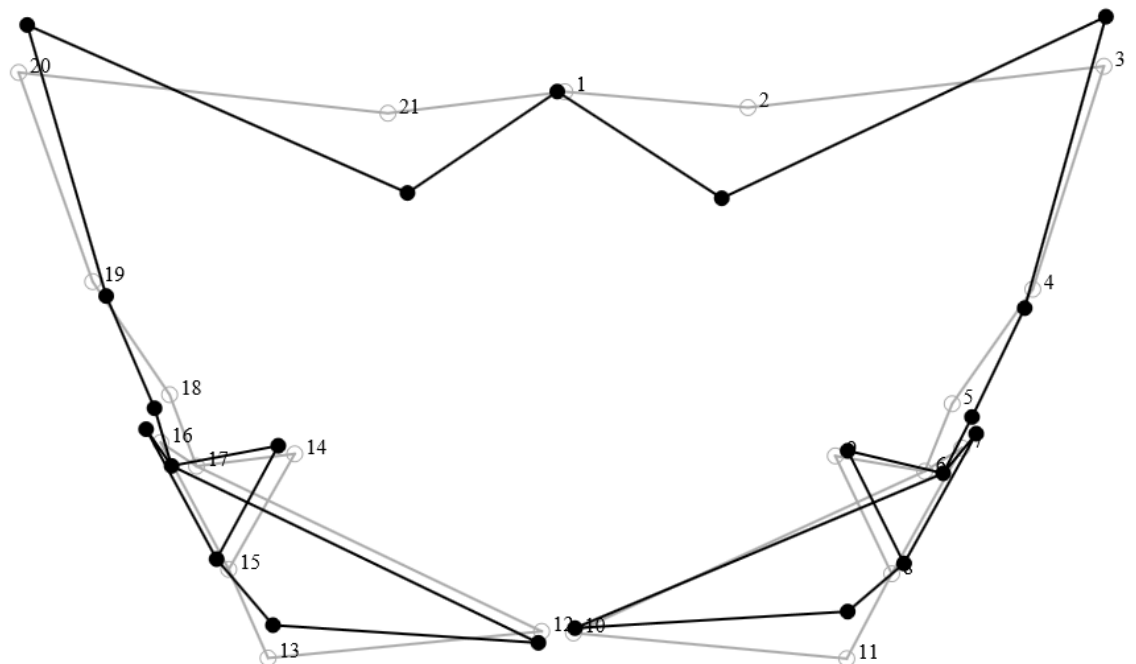


Figure 3.15: PC2 shape changes between females and males in the pelvis in the superior view, posterior is up (landmark numbers correspond to those in Table 1.1)

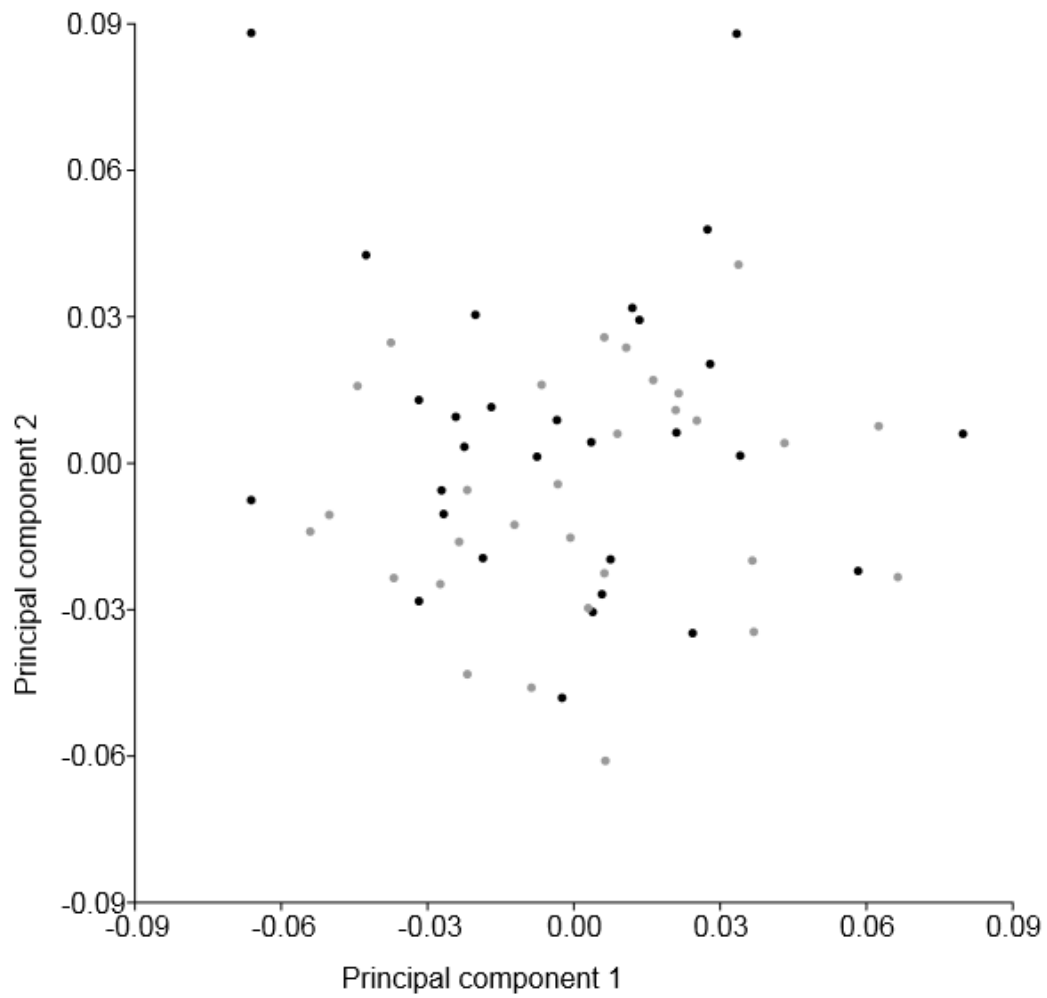


Figure 3.16: PC1 and PC2 graph for the femur in females (gray) and males (black)

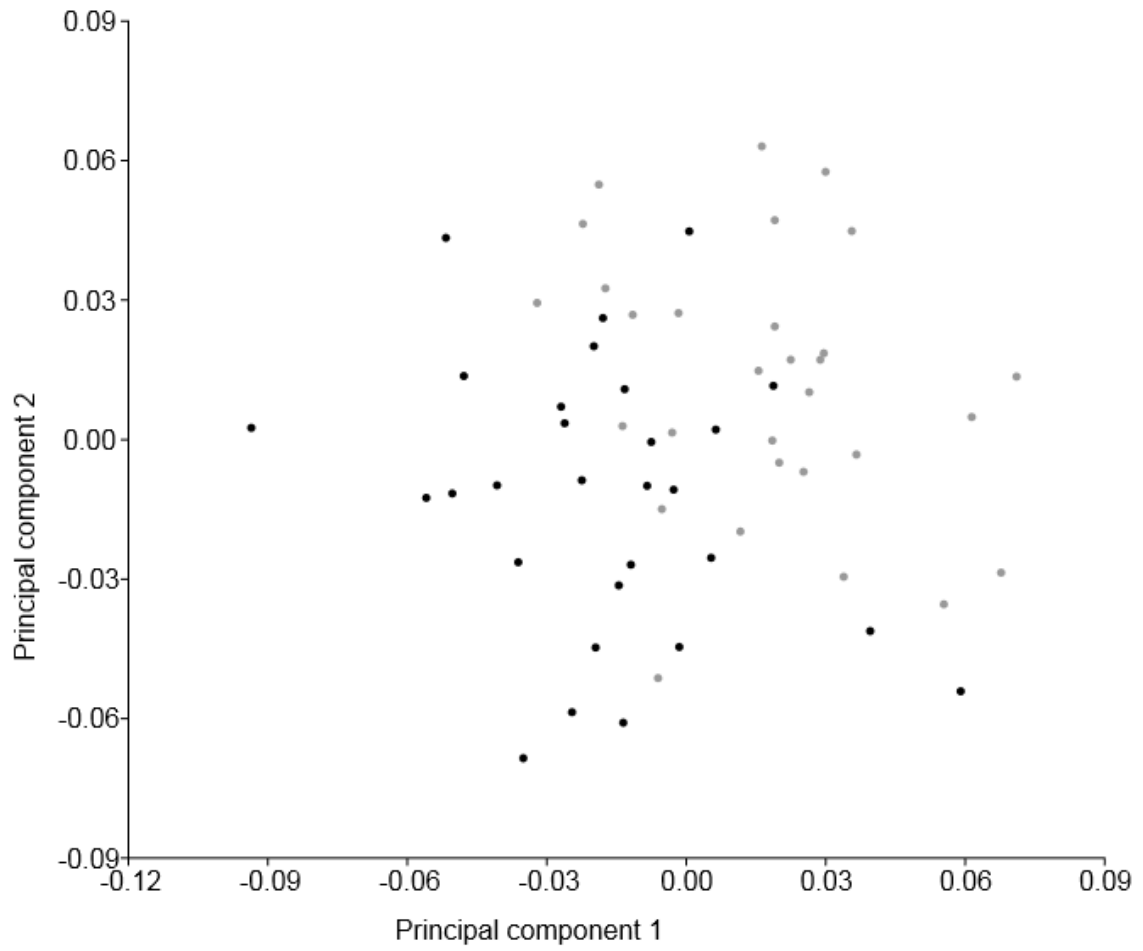


Figure 3.17: PC1 and PC2 graph for the pelvis in females (gray) and males (black)

The DFA with a stepwise procedure in SPSS was utilized with the sexually dimorphic variables of the femur to provide a statistical formula for sex estimation. Neck-shaft angle was removed as a variable during the stepwise procedure. The centroids for each group are 1.059 for males and -1.059 for females.

Table 2.6: Standardized canonical coefficients for the femur

Measurement	Coefficient
Bicondylar Angle	-0.380
Neck Length	.638
Biomechanical Neck Length	.551

Table 2.7: Classification results¹

Group	Males	Females	Total
Males	24	6	30
Females	3	27	30

¹ 85.0% of original grouped cases correctly classified.

Null Hypotheses Results Summary

Table 2.8 summarizes all null hypotheses of this thesis and the results of the research. All null hypotheses are rejected except for H₀₂: There is no significant sexual dimorphism in bi-iliac breadth.

Table 2.8: Summary of null hypotheses tested in this thesis

H₀	Statement of Null Hypothesis	Test Utilized	Result
H ₀₁	There is no significant sexual dimorphism in biacetabular breadth.	One-way ANOVA (Table 4, Figure 4.1)	Reject H ₀₁
H ₀₂	There is no significant sexual dimorphism in the bi-iliac breadth.	One-way ANOVA (Table 4)	Cannot reject H ₀₂
H ₀₃	There is no significant sexual dimorphism in the biomechanical neck length.	One-way ANOVA (Table 4, Figure 4.2)	Reject H ₀₃
H ₀₄	There is no significant sexual dimorphism in the femoral angle of version.	Mann-Whitney U (Table 5)	Reject H ₀₄
H ₀₅	There is no significant sexual dimorphism in overall femoral shape and morphology	Procrustes ANOVA and CPA (Figures 6.1 and 6.2)	Reject H ₀₅
H ₀₆	There is no significant sexual dimorphism in the neck-shaft angle.	One-way ANOVA (Table 4, Figure 4.3)	Reject H ₀₆
H ₀₇	There is no significant sexual dimorphism in the femoral bicondylar angle.	One-way ANOVA (Table 4, Figure 4.3)	Reject H ₀₇
H ₀₈	There is no significant sexual dimorphism in overall pelvic shape and morphology	Procrustes ANOVA and CPA (Figures 6.3-6.6)	Reject H ₀₈
H ₀₉	There is no significant sexual dimorphism in the acetabular angle of version.	Figures 6.5 and 6.6	Reject H ₀₉ (observed)
H ₀₁₀	There is no relationship between the biacetabular breadth and the femoral neck-shaft angle.	Pearson Correlation (Table 6, Figure 5.1)	Reject H ₀₁₀
H ₀₁₁	There is no relationship between the biacetabular breadth and the femoral bicondylar angle.	Pearson Correlation (Table 6, Figure 5.2)	Reject H ₀₁₁
H ₀₁₂	There is no relationship between the biomechanical neck length and the femoral bicondylar angle.	Pearson Correlation (Table 6, Figure 5.3)	Reject H ₀₁₂

CHAPTER IV

DISCUSSION

The purpose of this study was to examine the relationship between biacetabular breadth and the shape of the femur in American White males and females, and how this affects the pattern of sexual dimorphism in the femur. Femur size, shape, and angles are examined within a biomechanical framework using geometric morphometric methods to understand sex differences in femur morphology.

Significant sexual dimorphism was found in all the size measurements and angles, except for bi-iliac breadth. The MorphoJ GPA ANOVA results indicated that both the femur and pelvis display a significant level of sexual dimorphism in shape. This supports the idea that there is both size and shape sexual dimorphism in femoral morphology. Regarding bi-iliac breadth, Driscoll (2010) observed a secular decrease in bi-iliac breadth among Americans, and observed that these changes are also less biomechanically advantageous. That is, a more flared ilium provides a more mechanically efficient muscle attachment site and decreases loading on the femoral head (Delprete, 2006; Lovejoy, 1988). With the understanding that a narrowing pelvis may increase work load, males and females might accommodate this secular change differently during skeletal development. However, overall shape analysis of the pelvis displayed a more flared ilium for females (Figure 3.13).

While H_0 regarding bi-iliac sexual dimorphism could not be rejected, the PCA wireframes depicted a clearly flared pelvis, consistent with previous anatomical assessments (Netter, 2011). This suggests that while there is no significant difference in

overall width of the pelvis, that females have relatively more flared ilia. This is an important distinction because the ilia are the site of several large muscle attachments, and therefore their morphology is integral to the understanding of differences in the pelvis and lower extremities. A ratio of the anatomical length of the femur to the bi-iliac breadth also showed sexual dimorphism in the sample, with a p-value of <0.001 . The flared ilia and its relation to hip morphology will be discussed in more detail later in this chapter. In testing H_09 (no significant sexual dimorphism in the acetabular angle of version), Figures 3.14 (in particular) and 3.15 displayed a more anteverted acetabular position for females. This is consistent with previous research regarding female acetabular anteversion (Tohtz et al., 2010; Nakahara et al., 2011; Hetsroni et al., 2013). A more anteverted acetabulum affects an individual's range of motion in external rotation (Nakahara et al., 2011), thereby affecting gait and functional capacity.

The proximal femoral shape in Figures 3.10 and 3.11 is consistent with a smaller neck-shaft angle in males. The subtrochanteric points are also higher in males for PCA 1 (Figure 3.10), suggesting a possible sex variation in muscle attachment sites on the femur. The femoral condyles displayed sex variation differences (Figure 3.11). In the two epicondyle landmarks, 19 and 20, the vectors of female to male shape are consistent with a more narrow epicondylar breadth for females relative to their size. These results are consistent with Conley and colleagues (2007) who found that females displayed a reduced medial-lateral:anterior-posterior aspect ratio in the femoral condyles in the inferior view of the distal articular surface. To reduce the effects of size in this study, samples of the inferior view of the femur articulating surface shape were scaled to one anterior-posterior length to examine the condylar shape. The profile of the female

femoral condyles were more narrow and trapezoidal than square in comparison to males when viewed from the inferior articulating surface. The condylar articulation points for the tibia also display variation in Figure 3.12, perhaps relating to the observed bicondylar angle differences.

To help explain the significant shape variation in the femur, the relationship between biacetabular breadth and biomechanical angles was examined. Unexpectedly, while the bicondylar angle was also sexually dimorphic, females have an angle closer to 90 degrees than males. Tardieu and colleagues (2006) noted that the overall trend in sexual dimorphism in humans is for females to display a more acute bicondylar angle. This is attributed to the (usually) larger biacetabular breadth, and the fact that females generally have smaller femurs (in length and robusticity) than males within a population. Therefore a wider pelvis and shorter femur would necessitate a larger bicondylar angle for the distal femur to meet the center of gravity below the hip at the knee. Thus, since the biacetabular breadth is significantly sexually dimorphic in this sample, a larger bicondylar angle is expected in the female sample. But this assessment does not account for neck length or neck-shaft angle, shown to be an important factor in this research.

The available samples in most studies (Parsons, 1910; Walmsley, 1933; Heiple and Lovejoy, 1971; Tardieu et al., 2006) are either historical or are classified as modern without specific ranges of birth and death years provided. Driscoll (2010) and Wescott and Zaphro (2012) have observed secular changes in the pelvis and femur, respectively. More specifically, Wescott and Zephro (2012) note that secular change in Whites indicates differences in mechanical loading on the femur, and suggest that, “Since most methods for estimating biomechanical characteristics from the femur are based on

nineteenth century skeletal collections, it is crucial that we understand how secular changes may affect the interpretation of sex, stature, ancestry, and activity patterns in modern Americans.” Therefore, the association between biacetabular breadth and bicondylar angle may vary among cohorts.

The bicondylar angle observed in females is consistent with the other morphological trends of the femur in this sample. A positive relationship between the neck-shaft angle and bicondylar angle (Figure 3.7) indicates that a larger neck-shaft angle is associated with a greater bicondylar angle. The larger biacetabular breadth, and by extension a wider pelvis, is also correlated with a larger neck-shaft angle in this sample. Weidow (2006) found that a lower femoral offset and coxa valga (large neck-shaft angle) compensated for a wider pelvis in patients with and without osteoarthritis. A study by Atkinson et al. (2010) that controlled for population effects also pointed to a similar trend in sex variation with neck-shaft angles in a Caucasian (White) sample.

A larger neck-shaft angle creates a smaller lever arm by reducing biomechanical length of the femoral neck. A larger biacetabular breadth, and by extension a wider pelvis, is correlated with a larger neck-shaft angle in this sample. This smaller lever arm reduces the severity of the angle to which the distal femur articulates with the tibia to form the base of support. It increases the moment of the hip creating a less stable joint (Anderson and Trinkaus, 1998). The reduced lever arm is observable in the biomechanical length data of the femoral neck.

There is a negative relationship between bicondylar angle and biomechanical neck length (Figure 3.8). The dimensions of the ilium and biomechanical neck length are important in determining moment size, since the length between the two features affects

the length and attachments of the gluteus medius and tensor fascia latae (Ruff, 1995). In Figure 3.12, the female iliac blades flare more than the male individuals, and this is an observation acknowledged in other anatomical resources (Netter, 2011). Thus, the more flared ilia relative to the overall size of the os coxae in females helps to shorten the distance between the muscle attachment sites for the femur and ilium. Conversely, the more anteverted femur and acetabula observed in females would lengthen these same muscles and perhaps lead to a less stable joint.

Overall, greater femoral torsion in females is supported in biomechanical research, and by studies showing that females with femoral version were more likely to experience hip pain (Nakahara et al., 2011; Hetsroni et al., 2013). The female characteristics – smaller biomechanical neck, larger neck-shaft angle, greater torsion, and flared ilia – appear to be a biomechanical adaptation to the overall widening of the pelvis in the acetabulum, at least for modern White individuals.

The larger biomechanical neck length in males creates a larger moment and lever arm, possibly resulting in a more uneven pressure on the epiphyseal plates during development. The condylar epiphyseal plates respond to uneven pressure by adjusting the rate of growth, with the lateral condyle tending to grow more antero-posteriorly and the medial condyle growing in a more superio-inferior direction (Tardieu and Trinkaus, 1994). This would explain the smaller bicondylar angle in males. However, the correlation is likely more the result of interdependent growth than a simple cause and effect.

It is uncertain if this same relationship exists in other populations. Gilligan and colleagues (2013) examined neck-shaft angles from over 30 population groups worldwide

and noted no sex differences when considering all groups. In certain groups variation existed, but not all variation followed the same pattern. Multiple variables correlated with changes in the neck-shaft angle among populations, including differences in subsistence (hunting/gathering, agriculture, sedentary), and use of clothing. The neck-shaft angle was more tightly correlated with winter temperatures, with 20% of the variability explained by climate. This suggests that neck-shaft angle is more significantly affected by climate than other factors. That finding is consistent with the hypothesis based on Bergmann's rule that a lower neck-shaft angle is an adaption suited for a more robust frame to maintain body heat, rather than a more linear, gracile build suited for warmer climates. Activity level also correlated with the neck-shaft angle, but not as significantly as the thermal factors, and the findings were less divergent than the correlations reported by Anderson and Trinkaus (1998).

The unique contributions of winter temperature and thermal protection (clothing) yielded significant p-values of <0.001 and <0.05 , respectively in the Gilligan and colleagues (2013) study, acknowledging the significant contribution of cultural buffering to this morphological trait in humans. Increased protection from the environment with clothing and housing yielded an overall trend of less neck-shaft variability among populations of differing climates. Since population effects were not included in the analysis by Gilligan et al. (2013), it is uncertain what genetic influences are affecting the femoral shape. By controlling for population in this research, the question of ancestry-related trends in morphology can begin to be explored.

The ontogeny of the bicondylar angle and neck-shaft angle is directly tied to bipedal locomotion. Clear morphological changes occur at the onset of walking, and

individuals who never walk do not develop a bicondylar angle and have a neck-shaft angle greater than 150 degrees (Tardieu et al., 2006b). The biomechanical pressure on the femoral head and neck in an individual with a normal gait reduces the neck-shaft angle during growth. The valgus angle that forms for the knee to be in line with the center of gravity creates uneven pressure on the epiphyseal plates. Since pressure on the epiphyseal plates of the distal femur causes differential growth, if the neck-shaft angle is significantly affected by thermal conditions and cultural buffering as Gilligan et al. (2013) suggest, then a greater bicondylar angle in females may only exist when the environment and activity level permits a smaller neck-shaft angle to develop within a population.

Therefore, the DFA equation from this analysis, which accurately identified sex in 85% of individuals, should only be utilized within a known (or suspected) modern American White sample. The equation provides more accurate results for female than male femora, suggesting more variability within the male sample. This can be observed in Figures 3.1-3.4, displaying a wider variation within the male sample for all variables (as well as more outliers). With further examination of population differences, however, more aspects of shape compensation for pelvic breadth might become clearer.

Kurki (2013) noted certain trends in pelvic outlet area among populations. The size was less variable than the dimensions (length and width) of the outlet. Although this study found a large amount of variation in pelvic canal dimensions, female canal and noncanal dimensions were correlated across populations, so it is possible that dimorphism might be evident in other areas of the femur shape in groups other than modern American Whites. For example, a population group with no mean difference in neck-shaft angle

might demonstrate a greater dimorphism in torsion or bicondylar angle. The data in this thesis support a strong relationship between the neck-shaft angle and bicondylar angle. However, multiple populations should be examined to reveal any morphogenetic and/or environmental differences among groups that may create a different relationship in femur morphology.

Biomechanical and sports medicine studies thus far also failed to find a greater bicondylar angle in females. The observed sex differences in lower limb morphology- greater knee adduction and internal rotation in females- generally correlated with an increased risk for injury, especially knee injury. But, most sex differences in lower limb alignment could be corrected with neuromuscular training (Myer et al., 2013). More specifically, physical therapy regimens target individuals with knee injuries to align the knee and hip joints and correct likely causes of joint instability: muscle imbalance, poor posture, and/or ligament laxity (Hewett et al., 2013). Powers (2010) noted that females are more influenced by proximal causes for knee injury, such as hip adductor strength imbalances than males. The observations of this thesis, including the smaller biomechanical neck length for females, perhaps contribute to difficulties in maintaining muscle strength in these key areas.

However, it is important to note that the variation seen in this study are applicable only in American Whites and more research should be done to examine if other populations display similar trends. The medical literature is not consistent in controlling for population, as some articles, such as Conley et al. (2007) note sex variation but do not state parameters for ancestral population. Other articles concentrate on population-specific variation for arthroplasty or injury risk, but are solely focused on specific

surgical issues (Vaidya SV, Ranawat CS, Aroojis A, 2000; Kwak et al., 2007; Shelbourne et al., 2007).

While skeletal variation exists, the research conducted in this thesis demonstrates a clear correlation in the changes in femur morphology corresponding to bi-acetabular breadth. This highlights the necessity of examining all aspects of lower limb morphology when researching pathologies and shape variation. It is particularly important in regards to skeletal development, as early activity or inactivity can produce irreversible shape differences. The pelvic widening is a genetically predetermined, but the femur is quite responsive to the biomechanical stress. Therefore, skeletal genetic and phenotypic growth may not develop cohesively.

Conclusion

The 3D geometric morphometric analysis in this thesis illuminated the sexual dimorphism and variation in the pelvis and femur for modern American White individuals. The wider biacetabular breadth present in females correlated with a greater neck-shaft angle and smaller bicondylar angle. The flared ilia also present in females further illustrated the biomechanical adjustments in the widening pelvis.

The male sample presented a smaller neck-shaft angle and larger bicondylar angle, with a less flared ilia and wider femoral epicondyles. These factors create a larger lever arm on the femoral neck and reduce the moment about the hip for males, creating a more stable joint. Conversely, females have a less stable joint and likely have longer muscle attachments, particularly for individuals with femoral anteversion.

A more thorough understanding of lower limb morphology detailed in this research is relevant to multiple subdisciplines within anthropology. Human evolutionary

theory relies on a grasp of how genetic, environmental, and biomechanical influences affect skeletal variation. Bioarchaeological methods regularly employ shape and size variables when constructing past lifeways. And forensic anthropology utilizes modern samples of skeletal data when constructing biological profiles of unknown individuals. Now, anthropologists have more information regarding the variation and likely multifactorial mechanisms underlying lower limb variation with the methods and results detailed in this thesis.

The DFA equation in this thesis provides a good method for estimating sex in a known modern American White sample, especially in the event of some taphonomic damage. Further research could focus on expanding the sample to include other population groups for separate DFA equations. Other populations might display different variation patterns that might make this method more effective.

Beyond anthropology, general biomechanical and sports medicine research benefits from a more complete picture of the skeletal structure underlying sexual dimorphism. This will hopefully spur further inquiry about how this variation may affect other aspects of overall joint health and injury risk/prevention.

REFERENCES

- Albanese J, Eklics G, and Tuck A. 2008. A metric method for sex determination using the proximal femur and fragmentary hipbone. *J. Forensic Sci.* 53:1283–8.
- Anderson JY, and Trinkaus E. 1998. Patterns of sexual, bilateral and interpopulational variation in human femoral neck-shaft angles. *J. Anat.* 192:279–285.
- Atkinson HD, Johal KS, Willis-Owen C, Zadow S, and Oakeshott RD. 2010. Differences in hip morphology between the sexes in patients undergoing hip resurfacing. *J. Orthop. Surg. Res.* 5:76–80.
- Auerbach BM, and Ruff CB. 2010. Stature estimation formulae for indigenous North American populations. *Am. J. Phys. Anthropol.* 141:190–207.
- Binder D, and Brown-cross D. 2001. Peak torque, total work and power values when comparing individuals with Q-angle differences. *Isokinet. Exerc. Sci.* 9:27–30.
- Bookstein, FL. 1991. *Morphometric tools for landmark data: geometry and biology.* Cambridge Univ. Press: New York
- Byl T, Cole JA, and Livingston LA. 2000. What Determines the Magnitude of the Q Angle ? A Preliminary Study of Selected Skeletal and Muscular Measures. *J. Sport Rehabil.* 9:26–35.
- Bytheway J a, and Ross AH. 2010. A geometric morphometric approach to sex determination of the human adult os coxa. *J. Forensic Sci.* 55:859–64.
- Conley S, Rosenberg A, and Crowninshield R. 2007. The female knee: anatomic variations. *J. Am. Acad. Orthop. Surg.* 15 Suppl 1:S31–6.
- Driscoll KRD. 2010. *Secular Change of the Modern Human Bony Pelvis : Examining Morphology in the United States using Metrics and Geometric Morphometry.* Dissertation. University of Tennessee-Knoxville.
- Fabeck L, Tolley M, Rooze M, and Burny F. 2002. Theoretical study of the decrease in the femoral neck anteversion during growth. *Cells Tissues Organs* 171:269–75.
- Gilligan I, Chandraphak S, and Mahakkanukrauh P. 2013. Femoral neck-shaft angle in humans: variation relating to climate, clothing, lifestyle, sex, age and side. *J. Anat.* 223:133–51
- Heiple K, and Lovejoy C. 1971. The distal femoral anatomy of *Australopithecus*. *Am. J. Phys. Anthropol.* 35:75–84.

- Hetsroni I, Dela Torre K, Duke G, Lyman S, and Kelly BT. 2013. Sex differences of hip morphology in young adults with hip pain and labral tears. *Arthroscopy* 29:54–63.
- Hewett TE, Di Stasi SL, and Myer GD. 2013. Current concepts for injury prevention in athletes after anterior cruciate ligament reconstruction. *Am. J. Sports Med.* 41:216–24.
- Holliday TW, Hutchinson VT, Morrow MMB, and Livesay G. 2010. Geometric morphometric analyses of hominid proximal femora: taxonomic and phylogenetic considerations. *Homo* 61:3–15.
- Kimmerle EH, Jantz RL, Konigsberg LW, and Baraybar JP. 2008. Skeletal estimation and identification in American and Eastern European populations. *J. Forensic Sci.* 53(3):524–532.
- Kurki HK. 2007. Protection of Obstetric Dimensions in a Small-Bodied Human Sample. 1165:1152–1165.
- Kurki HK. 2011. Pelvic dimorphism in relation to body size and body size dimorphism in humans. *J. Hum. Evol.* 61:631–43.
- Kurki HK. 2013. Skeletal variation in the pelvis and limb skeleton of humans: does stabilizing selection limit female pelvis variation? *Am. J. Human Bio.* 25:795–802.
- Kwak DS, Surendran S, Pengatteeeri YH, Park SE, Choi KN, Gopinathan P, Han SH, and Han CW. 2007. Morphometry of the proximal tibia to design the tibial component of total knee arthroplasty for the Korean population. *Knee* 14:295–300.
- Mitteroecker P, and Gunz P. 2009. Advances in Geometric Morphometrics. *Evol. Biol.* 36:235–247.
- Myer GD, Sugimoto D, Thomas S, and Hewett TE. 2013. The influence of age on the effectiveness of neuromuscular training to reduce anterior cruciate ligament injury in female athletes: a meta-analysis. *Am. J. Sports Med.* 41:203–15.
- Nakahara I, Takao M, Sakai T, Nishii T, Yoshikawa H, and Sugano N. 2011. Gender differences in 3D morphology and bony impingement of human hips. *J. Orthop. Res.* 29:333–9.
- Netter FH. 2011. *Atlas of Human Anatomy*. 5th ed. Philadelphia: Saunders Elsevier.
- Parsons F. 1910. The Characters of the English Thighbone. *J. Anat. Physiol.* 48:238–267.
- Phenice T. 1969. A newly developed visual method of sexing the os pubis. *Am. J. Phys. Anthropol.* 30:297–302.

- Powers CM. 2010. The influence of abnormal hip mechanics on knee injury: a biomechanical perspective. *J. Orthop. Sports Phys. Ther.* 40:42–51.
- Ruff CB. 1995. Biomechanics of the hip and birth in early Homo. *Am. J. Phys. Anthropol.* 98:527–74.
- Salenius P, and Vankka E. 1975. The development of the tibiofemoral angle in children. *J. Bone Jt. Surg.* 57:259–61.
- Scheuer L, and Black S. 2000. *Developmental Juvenile Osteology*. 1st ed. Oxford: Elsevier Ltd.
- Shelbourne KD, Gray T, and Benner RW. 2007. Intercondylar notch width measurement differences between African American and white men and women with intact anterior cruciate ligament knees. *Am. J. Sports Med.* 35:1304–7.
- Spradley MK, and Jantz RL. 2011. Sex estimation in forensic anthropology: skull versus postcranial elements. *J. Forensic Sci.* 56:289–96.
- Srivastava R, Saini V, Rai RK, Pandey S, and Tripathi SK. 2011. A study of sexual dimorphism of the femur among Northern Indians. *J. Forensic Sci.* 57(1):19-23.
- Stem ES, O'Connor MI, Kransdorf MJ, and Crook J. 2006. Computed tomography analysis of acetabular anteversion and abduction. *Skeletal Radiol.* 35:385–9.
- Stull KE, and Godde K. 2013. Sex estimation of infants between birth and one year through discriminant function analysis of the humerus and femur. *J. Forensic Sci.* 58(1):13-20/
- Tardieu C, Glard Y, Garron E, Boulay C, Jouve J-L, Dutour O, Boetsch G, and Bollini G. Relationship between formation of the femoral bicondylar angle and trochlear shape. Independence of diaphyseal and epiphyseal growth. *Am. J. Phys. Anthropol.*
- Tardieu C, Glard Y, Garron E, Boulay C, Jouve J-L, Dutour O, Boetsch G, and Bollini G. 2006. Relationship between formation of the femoral bicondylar angle and trochlear shape: independence of diaphyseal and epiphyseal growth. *Am. J. Phys. Anthropol.* 130:491–500.
- Tardieu C, and Trinkaus E. 1994. Early ontogeny of the human femoral bicondylar angle. *Am. J. Phys. Anthropol.* 95:183–95.
- Tardieu C. 2010. Development of the human hind limb and its importance for the evolution of bipedalism. *Evol. Anthropol. Issues, News, Rev.* 19:174–186.
- Tise ML, Spradley MK, and Anderson BE. 2012. Postcranial sex estimation of individuals considered Hispanic. *J. Forensic Sci.* 58S1:S9-S14.

- Tohtz SW, Sassy D, Matziolis G, Preininger B, Perka C, and Hasart O. 2010. CT evaluation of native acetabular orientation and localization: sex-specific data comparison on 336 hip joints. *Technol. Health Care* 18:129–36.
- Trotter M, and Gleser C. 1952. Estimation of stature of long bones from American whites and Negroes. *Am. J. Phys. Anthropol.* 10:463–514.
- Vaidya SV, Ranawat CS, Aroojis A LN. 2000. Anthropometric measurements to design total knee prostheses for the Indian population. *J Arthroplast.* 15:79–85.
- Walmsley BYT. 1933. The vertical axes of the femur. *J. Anat.* 67:284–300.
- Weidow J. 2006. Lateral osteoarthritis of the knee. *Acta Orthop.* 77:2–44.
- Wescott DJ, and Cunningham DL. 2013. Temporal changes in Arikara femoral torsion. In: *American Journal of Physical Anthropology*.
- Wescott DJ, and Zephro L. 2012. Secular change in the femur. In: *American Journal of Physical Anthropology* 147 (S54). p 308.